Contribution from the Department of Chemistry,
Massachusetts Institute of Technology, Cambridge, Massachusetts 02139

Synthesis and Characterization of [d(ApGpGpCpCpT)]$_2$ and Its Adduct with the Anticancer Drug *cis*-Diamminedichloroplatinum(II)

John P. Caradonna and Stephen J. Lippard*

Received August 21, 1987

The self-complementary deoxyribohexanucleoside pentaphosphate d(ApGpGpCpCpT) and the major product of its reaction with the antitumor drug *cis*-diamminedichloroplatinum(II) (*cis*-DDP) have been characterized by high-resolution ^{1}H and ^{31}P NMR spectroscopy. Temperature-dependence studies of the amino, imino, and nonexchangeable base protons of [d(ApGpGpCpCpT)]$_2$ indicate that the oligonucleotide adopts a duplex structure in solution with frayed terminal A(1)·T(6) base pairs. The duplex exhibits a noncooperative melting profile; the terminal base pairs melt 10–15 °C lower than the inner [–GpGpCpC–]$_2$ core (T_M = 60.0 ± 3.0 °C). The nonexchangeable base protons were assigned by two-dimensional nuclear Overhauser effect and homonuclear chemical shift correlation experiments. Each 2′-deoxyribose moiety has $\sum(J_{H1'H2'} + J_{H1'H2''})$ values of 14.0 ± 1.0 Hz throughout the temperature (2–65 °C) and pD (3.2–10.8) ranges investigated, characteristic of a B-DNA type (C2′ endo) structure. The reaction of *cis*-DDP with [d(ApGpGpCpCpT)]$_2$ was carried out under conditions in which the oligonucleotide was in duplex form, allowing the possible formation of interstrand, intrastrand, or intrabase adducts. Only the second of these three possibilities was observed. The platinum binding site was determined by investigating the ^{1}H NMR behavior of the nonexchangeable base protons of both the unmodified and modified oligonucleotides as a function of pD. The pK_a values of both guanine N1 protons decreased from 10 to 8 upon binding of platinum. All nonexchangeable base protons shifted to lower fields, with both guanine H8 resonances exhibiting the characteristic 0.3–0.9 ppm downfield shift. These results demonstrate that the isolated product contains an intrastrand cross-link between two N7 atoms of adjacent guanosine residues, the most prevalent adduct formed by *cis*-DDP in tumor cells. No evidence was found for the other commonly occurring adduct, an intrastrand d(ApG) cross-link. The data further indicate that *cis*-[Pt(NH$_3$)$_2$[d(ApGpGpCpCpT)-*N7-G(2),N7-G(3)*]] adopts a single-stranded, base-destacked, coil structure that is unable to form a Watson–Crick duplex with itself.

Introduction

The discovery of the antitumor properties of *cis*-[Pt(NH$_3$)$_2$Cl$_2$] (*cis*-DDP)[1] has stimulated intensive efforts in the fields of inorganic, biological, and medicinal chemistry toward elucidating the mechanism of action of this drug. There is considerable evidence that *cis*-DDP exerts its antineoplastic effects by binding to DNA and inhibiting replication in the cancer cell.[2-4] It is therefore of interest to understand at the molecular level how this relatively simple compound perturbs local DNA conformation, for such structural alterations translate ultimately into biological activity.

Over the past few years, high-resolution ^{1}H NMR spectroscopic studies have been carried out to provide insight into the interactions of *cis*-[Pt(NH$_3$)$_2$Cl$_2$] with DNA.[5-12] Recent X-ray crystallographic[13,14] and molecular mechanics[15-17] studies have also contributed to our understanding of the structural chemistry of *cis*-DDP with oligonucleotides. A comprehensive review of this material is given elsewhere.[18]

The present investigation of the reaction between *cis*-DDP and the self-complementary deoxyribohexanucleoside pentaphosphate [d(ApGpGpCpCpT)]$_2$ was undertaken in part to ascertain whether the major adduct would consist of an intrastrand, interstrand, or intrabase cross-link. Each of these binding modes has been proposed as an important cytotoxic lesion of *cis*-DDP on DNA.[4] In addition, the chosen sequence provides the first opportunity to characterize reaction products of *cis*-DDP with a duplex oligonucleotide containing all the major known and postulated putative drug binding sites, namely, d(GpG) and d(ApG) (intrastrand),[19] d(GpC)·d(CpG) (interstrand),[20] and dG[N7-O6] (intrabase N7-O6 chelate).[21] Moreover, since the adducts of the chemotherapeutically inactive *trans*-DDP isomer of [d(ApGpGpCpCpT)]$_2$ have been characterized,[22] this investigation provides an excellent opportunity to compare directly differences in DNA binding of these two isomers. Finally, detailed examination of the *cis*-DDP adduct of [d(ApGpGpCpCpT)]$_2$ is of particular interest in conjunction with recently developed methodology for constructing site-specifically platinated intact viral genomes. The initial such biological probe contains the *cis*-DDP adduct of d(TpCpTp*ApGpGpCpCpT*pTpCpT), an oligonucleotide in which the title hexamer is embedded.[23]

In this paper, we report the synthesis and complete ^{1}H and ^{31}P NMR spectroscopic characterization of the duplex oligonucleotide [d(ApGpGpCpCpT)]$_2$ and the product of its reaction with *cis*-DDP, *cis*-[Pt(NH$_3$)$_2$[d(ApGpGpCpCpT)-*N7-G(2),N7-G(3)*]]. A

(1) Abbreviations used in this article are as follows: *cis*-DDP, *cis*-diamminedichloroplatinum(II); EDTA, ethylenediaminetetraacetate; DEAE, diethylaminoethyl; HPLC, high-performance liquid chromatography; SAX, strong anion exchange; TMA, tetramethylammonium; TMP, trimethyl phosphate; NMR, nuclear magnetic resonance; NOE, nuclear Overhauser effect; Pt/N, platinum-to-nucleotide ratio. Asterisks denote platination sites in oligonucleotide adducts.

(2) Roberts, J. J. *Adv. Inorg. Biochem.* **1981**, *3*, 274–332.
(3) Cleare, M. J.; Hydes, P. C. *Met. Ions. Biol. Syst.* **1980**, *11*, 1–62.
(4) Pinto, A. L.; Lippard, S. J. *Biochim. Biophys. Acta* **1985**, *780*, 167–180.
(5) Chottard, J.-C.; Girault, J.-P.; Chottard, G.; Lallemand, J.-Y.; Mansuy, D. *J. Am. Chem. Soc.* **1980**, *102*, 5565–5572.
(6) Girault, J.-P.; Chottard, G.; Lallemand, J.-Y.; Chottard, J.-C. *Biochemistry* **1982**, *21*, 1352–1356.
(7) Marcelis, A. T. M.; Canters, G. W.; Reedijk, J. *Recl. Trav. Chim. Pays-Bas* **1981**, *100*, 391–392.
(8) Marcelis, A. T. M.; den Hartog, J. H. J.; Reedijk, J. *J. Am. Chem. Soc.* **1982**, *104*, 2664–2665.
(9) den Hartog, J. H. J.; Altona, C.; Chottard, J.-C.; Girault, J.-P.; Lallemand, J.-Y.; Le Leeuw, F. A. A. M.; Marcelis, A. T. M.; Reedijk, J. *Nucleic Acids Res.* **1982**, *10*, 4715–4730.
(10) den Hartog, J. H. J.; Altona, C.; van Boom, J. H.; van der Marel, G. A.; Haasnoot, C. A. G.; Reedijk, J. *J. Am. Chem. Soc.* **1984**, *106*, 1528–1530.
(11) den Hartog, J. H. J.; Altona, C.; van Boom, J. H.; Reedijk, J. *FEBS Lett.* **1984**, *176*, 393–397.
(12) van Hemelryck, B.; Guittet, E.; Chottard, G.; Girault, J.-P.; Huynh-Dinh, T.; Lallemand, J.-Y.; Igolen, J.; Chottard, J.-C. *J. Am. Chem. Soc.* **1984**, *106*, 3037–3039.
(13) Sherman, S. E.; Gibson, D.; Wang, A. H.-J.; Lippard, S. J. *Science (Washington, D.C.)* **1985**, *230*, 412–417.
(14) Admiraal, G.; van der Veer, J. L.; de Graaff, R. A. G.; den Hartog, J. H. J.; Reedijk, J. *J. Am. Chem. Soc.* **1987**, *109*, 592–594.
(15) Kozelka, J.; Petsko, G. A.; Lippard, S. J.; Quigley, G. J. *J. Am. Chem. Soc.* **1985**, *107*, 4079–4081.
(16) Kozelka, J.; Petsko, G. A.; Quigley, G. J.; Lippard, S. J. *Inorg. Chem.* **1986**, *25*, 1075–1077.
(17) Kozelka, J.; Archer, S.; Petsko, G. A.; Lippard, S. J.; Quigley, G. J. *Biopolymers* **1987**, *26*, 1245–1271.
(18) Sherman, S. E.; Lippard, S. J. *Chem. Rev.* **1987**, *87*, 1153–1181.
(19) Fichtinger-Schepman, A. M. J.; van der Veer, J. L.; Lohman, P. H. M.; Reedijk, J. *Proc. Natl. Acad. Sci. U.S.A.* **1982**, *78*, 7010–7014.
(20) Eastman, A. *Biochemistry* **1985**, *24*, 5027–5032.
(21) Rosenberg, B. *Biochimie* **1978**, *60*, 859–867.
(22) Lepre, C. A.; Strothkamp, K. G.; Lippard, S. J. *Biochemistry* **1987**, *26*, 5651–5657.
(23) Pinto, A. L.; Naser, L. J.; Essigmann, J. M.; Lippard, S. J. *J. Am. Chem. Soc.* **1986**, *108*, 7405–7407.

0020-1669/88/1327-1454$01.50/0

preliminary report of a part of this work appeared previously.[24]

Experimental Section

Materials and Methods. Oligonucleotide Synthesis. Solvents and reagents were of the highest grade available commercially and were further purified and dried by standard methods.[25] The deoxyribohexanucleoside pentaphosphate d(ApGpGpCpCpT) was synthesized by the solid-phase phosphotriester method.[26] Bulk purification of the crude deprotected oligonucleotide was carried out by anion-exchange chromatography (Whatman, DEAE-cellulose, 20 × 1.5 cm), with use of a linear gradient (low buffer, 50 mM $(Et_3NH)(HCO_3)$, 20% EtOH, pH 7.5; high buffer, 0.5 M $(Et_3NH)(HCO_3)$, 20% EtOH, pH 7.5) to separate failure sequences from the desired product. Fractions containing the major product were pooled and lyophilized to remove most of the excess salt. Sample purity was verified by both anion-exchange (Partisil 10 SAX; 25 cm × 9.8 mm semipreparative column; linear gradient 0–30% B; solvent A, 6:4 1 mM phosphate formamide/H_2O, pH 7.5; solvent B, 6:4 300 mM phosphate formamide/H_2O, pH 7.5; 40 min; 3 mL/min) and reverse-phase HPLC, with a Waters dual-pump system.[24] Residual Et_3NH^+ was eliminated by cation-exchange chromatography (Bio-Rad AG-50W, NH_4^+ form, 25 × 0.75 cm). The lyophilized NH_4^+ salt of [d(ApGpGpCpCpT)]$_2$ was stored over desiccant at −20 °C.

The extinction coefficient of [d(ApGpGpCpCpT)]$_2$ was determined by treating an aliquot of the oligonucleotide (A_{260} = 2.135 ODU) with a saturated solution of twice-recrystallized 3,5-diaminobenzoic acid dihydrochloride (65 °C, 45 min) and measuring the fluorescence at 500 nm (420-nm excitation). Total nucleoside concentration was obtained by comparing these results to a standard curve generated from calf thymus DNA (A_{260}/A_{280} = 1.81).[27]

Reaction of *cis*-DDP with [d(ApGpGpCpCpT)]$_2$. *cis*-$[Pt(NH_3)_2Cl_2]$ was prepared according to literature methods[28] and recrystallized three times from 0.1 N HCl. The ammonium salt of [d(ApGpGpCpCpT)]$_2$ was allowed to react with *cis*-DDP in 1:2 (one platinum complex per strand), 1:1.25 and 1:1 (one platinum complex per duplex) molar ratios. All reactions were carried out at 37 °C in unbuffered deionized distilled H_2O (pH 6.0–6.7) for 96–144 h. The reaction mixture was not monitored at earlier time points for the possible formation of reactive intermediates, since our interest was to identify and characterize stable final products. Solution concentrations ranged from 0.33 to 3.33 mM strand with no discernable effect on product distribution. Isolation of the reaction products was accomplished by methods described above for [d(ApGpGpCpCpT)]$_2$. The ammonium salt of the platinated adduct was stored over desiccant at −20 °C.

Instrumentation. Platinum atomic absorption spectroscopy was performed on a Perkin-Elmer 2380 instrument, using an HGA 400 graphite furnace. All UV spectroscopic measurements were obtained on a Varian Cary 118C instrument, using jacketed 1-cm quartz cells thermostated by a Lauda constant-temperature bath.

NMR Sample Preparation. Typically, 80–90 A_{260} units of [d(ApGpGpCpCpT)]$_2$ or its *cis*-DDP adduct was used for ^{1}H NMR experiments; 350–400 A_{260} units was used for ^{31}P NMR studies. Prior to each experiment, the samples were passed through a desalting column (Sephadex G-10, 50 × 0.5 cm) and then through a Chelex-100 column (10 × 0.5 cm) to remove paramagnetic impurities. All UV-absorbing fractions were pooled, lyophilized, and dissolved in 350 μL of 0.1 M phosphate buffer, pH 7.4, containing 0.1 mM Na_2EDTA, except for those samples used for pH titration studies (no buffer) or exchangeable proton studies (vide infra). Tetramethylammonium chloride (TMA, δ = 3.180) was added as the internal standard. The samples were then lyophilized to dryness and coevaporated three times in 99.8% D_2O (Aldrich) before being dissolved in 350 μL of 99.998% D_2O (Stohler Isotopes, Inc.). Trimethyl phosphate (TMP, δ = 0.0) was used as the internal standard for ^{31}P NMR experiments.

The sample used in the T_1 study was deoxygenated by three freeze–pump–thaw cycles and sealed in an NMR tube under a N_2 atmosphere. Exchangeable base proton NMR studies required the sample to be dissolved in either 3/2 v/v H_2O/MeOH, 90% H_2O/10% D_2O, 100 mM phosphate, 1 mM Na_2EDTA, pH 7.4 ([d(ApGpGpCpCpT)]$_2$) or 90% H_2O/10% D_2O, 100 mM phosphate, 1 mM Na_2EDTA, pH 7.4 (*cis*-DDP adduct).

NMR Instrumentation and Procedures. Temperature regulation (±0.1 °C) was achieved by using the Bruker B-VT 1000 unit. Temperature calibration was performed between −15 and +30 °C by using neat MeOH and between +30 and +95 °C with ethylene glycol. Calibration curves were supplied by Bruker.

Temperature- and pH-dependent proton NMR and spin–lattice relaxation measurements were performed on a Bruker WM-300 wide-bore instrument with a 5-mm probe. Typically, 512 transients with a spectral width of 2250 Hz, from 16K complex data points, were averaged by a Bruker Aspect 2000 data system. Spectra were recorded with a 45° tip angle and a 4-s repetition time. Gaussian window techniques were routinely applied to improve spectral resolution.

The sample pH was adjusted with 1–5 μL aliquots of 1.0 N NaOD or DCl (Stohler Isotopes, Inc.) and measured with a Radiometer-Copenhagen type 100C pH meter (London Company) both before and after data accumulation. Differences of less than 0.05 pH unit were observed for all points. Measurements were corrected for deuterium effects by pD = pH + 0.4.[29] Studies with [d(ApGpGpCpCpT)]$_2$ were performed at 30 °C while those with *cis*-DDP-modified d(ApGpGpCpCpT) were carried out at 70 °C to enhance resolution.

Spin–lattice relaxation data were collected by using the $(\pi-\tau-\pi/2-A_t-D)_n$ nonselective inversion-recovery pulse sequence.[30] A series of 24 increments was used, ranging from 0.1 to 6.5 s with 11–14 τ values between $0.3T_1$ and $1.5T_1$ and 2–3 infinity points ($\tau \geq 5T_1$). The π and $\pi/2$ pulses were determined prior to each experiment by both the 360° null and 180° dispersion techniques.[31] Long-term NMR drift effects were minimized by accumulating 16 scans per τ value and recycling through the variable-delay list until 320 scans per τ value had been collected (20 cycles). A delay time of 9 s was used between pulse sequences ($A_t + D \geq 7T_1$). A locally written exponential regression algorithm was used to fit the data to the expression $I_\tau = C_1 + C_2 \exp(-\tau/T_1)$ in order to evaluate the possible effects of imperfect π and $\pi/2$ pulses.[31]

The oligonucleotide [d(ApGpGpCpCpT)]$_2$ in 90% H_2O/10% D_2O was studied over a temperature range by using water suppression techniques on a Bruker WM-360 instrument at The University of Pennsylvania Mid-Atlantic Regional NMR Facility. The Redfield 2–1–4–1–2 pulse sequence was employed,[32] by using a tailored pulse of 1700 μs to observe the region downfield of the null point (H_2O resonance, 19.1–5.2 ppm). Typically, 256 scans were collected, by using a 5000-Hz sweep width and 16K complex data points. Analogous experiments with *cis*-DDP-modified d(ApGpGpCpCpT) were carried out on a high-field 500-MHz spectrometer[33] at the Francis Bitter National Magnet Laboratory, using the time-shared long pulse sequence (TSLP).[34] Accumulation of 512 scans at 2 °C was performed by using a 7500-Hz sweep width and 8K complex data points. Resolution enhancement techniques were applied throughout these experiments.

Temperature-dependent ^{31}P NMR studies were recorded on a Bruker WM-500 instrument operating at 202 MHz at the Yale University Northeast Regional NMR Facility. An Aspect 2000A computer averaged 125 free induction decays, accumulated with a 30° tip angle and a total repetition time of 4.5 s. Sweep widths of 15 500 Hz and 16K complex data points gave a digital resolution of 1.89 Hz/point. Heteronuclear proton broad-band decoupling (1 W) and low-pass filters were used throughout the experiment. Lorentzian window functions were applied to improve the signal-to-noise ratio.

COSY and pure absorption NOESY experiments were performed at the Francis Bitter National Magnet Laboratory on a 500-MHz instrument. The COSY experiments were performed on nonspinning samples at 25 °C,[35] by using the sequence $[\pi/2-t_1-\pi/2-\text{acq}]_n$. Typically, the data sets consisted of 1024 data points over a sweep width of 3800 Hz in the t_2 dimension and 512 points in the t_1 dimension; the resulting matrix was processed with a Gaussian window function (4 Hz) in the two dimensions and zero-filled in the f_1 dimension to 1024 points. Both symmetrized and unsymmetrized contour maps were used. In the NOESY experiments, presaturation for 1800 ms at the residual HOD frequency preceded the pulse sequence. Mixing times of 200, 250, 275, and 300 ms were used.

(24) Caradonna, J. P.; Lippard, S. J.; Gait, M. J.; Singh, M. *J. Am. Chem. Soc.* **1982**, *104*, 5793–5795.
(25) Perrin, D. D.; Armarega, W. L. F.; Perrin, D. R. In *Purification of Laboratory Chemicals*, 2nd ed.; Pergamon: New York, 1980.
(26) Gait, M. J. In *Oligonucleotide Synthesis. A Practical Approach*; Gait, M. J., Ed.; IRL: Washington, DC, 1984; Chapter 1.
(27) Thomas, P. S.; Farquhar, M. N. *Anal. Biochem.* **1978**, *89*, 35–44.
(28) Dhara, S. C. *Indian J. Chem.* **1970**, *8*, 193–194.
(29) Glasoe, P. K.; Long, F. A. *J. Phys. Chem.* **1960**, *64*, 188–190.
(30) Vold, R. L.; Waugh, J. S.; Klein, M. P.; Phelps, D. E. *J. Chem. Phys.* **1968**, *48*, 3831–3832.
(31) Martin, M. L.; Delpuech, J.-J.; Martin, G. J. In *Practical NMR Spectroscopy*; Heyden: London, 1980.
(32) Redfield, A. G.; Kunz, S. D.; Ralph, E. K. *J. Magn. Reson.* **1975**, *19*, 114–117.
(33) Williams, J. E. C.; Neuringer, L. J.; Bobrov, E.; Weggel, R.; Ruben, D. J.; Harrison, W. G. *Rev. Sci. Instrum.* **1981**, *52*, 649–656.
(34) Wright, J. M.; Feigon, J.; Denny, W.; Leupin, W.; Kearns, D. R. *J. Magn. Reson.* **1981**, *45*, 514–519.
(35) Mehlkopf, A. F.; Korbee, D.; Tiggelman, T. A.; Freeman, R. *J. Magn. Reson.* **1984**, *58*, 315–323.

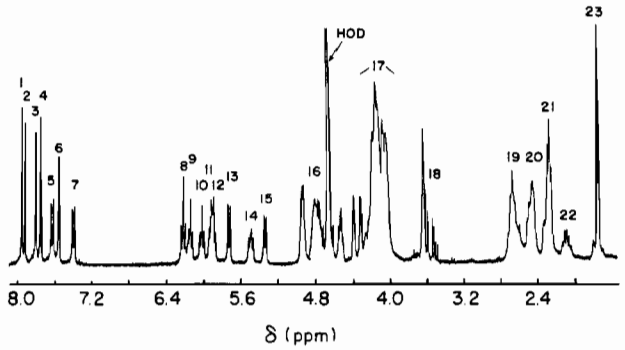

Figure 1. 300-MHz ^{1}H NMR spectrum of the nonexchangeable protons of 2.24 mM [d(ApGpGpCpCpT)]$_2$ (duplex concentration) in a solution containing 100 mM potassium phosphate buffer at pD 7.8 and 35 °C. The nonexchangeable base protons are located between 8.0 and 7.2 ppm, while the H1′ and cytosine H5 protons are found between 6.3 and 5.2 ppm. Resonance assignments are given in Table I.

All data were processed on a VAX 750 computer, using locally written programs.[36]

Results

Synthesis of [d(ApGpGpCpCpT)]$_2$ and *cis*-[Pt(NH$_3$)$_2$[d-(ApGpGpCpCpT)]. The solid-phase phosphotriester synthesis of d(ApGpGpCpCpT) (250 mg of resin, 84.4 μmol/g, 21.1-μmol scale) yielded 580 A_{260} units of oligonucleotide after bulk purification of the reaction mixture by anion-exchange chromatography. This material was homogeneous by both reverse-phase and anion-exchange HPLC, obviating the need for further purification.

Total DNA analysis[27] of an aliquot of [d(ApGpGpCpCpT)]$_2$ allowed the extinction coefficient at 25 °C to be calculated as $\epsilon_{260} \simeq 57\,400$ M^{-1} cm^{-1} per strand. This experimental value agrees with the extinction coefficient estimated by the nearest-neighbor approximation[37] for single-stranded DNA, $\epsilon_{260} = 56\,200$ M^{-1} cm^{-1}.

The reaction between *cis*-[Pt(NH$_3$)$_2$Cl$_2$] and [d-(ApGpGpCpCpT)]$_2$ was performed under conditions in which greater than 95% of the [–GpGpCpC–]$_2$ core exists in the duplex state. Only one major product, eluting as a trianion, was observed during purification by anion-exchange chromatography, regardless of the duplex oligonucleotide-to-platinum ratio (1:2, 1:1.25, and 1:1) or concentration (0.33–3.33 mM) used. The platinated product was homogeneous by reverse-phase HPLC analysis. Although the ammonium form of the oligonucleotide was used in the reaction with *cis*-DDP, the product profile showed no evidence of monofunctional platinated species such as those resulting from the use of NH_3 to trap platinum monodentate oligonucleotide intermediates.[38] In the case of the 1:1 reaction, the main platinated adduct and unreacted oligonucleotide accounted for greater than 95% of the total optical density at 254 nm, as estimated from peak areas obtained from reverse-phase HPLC analysis. No UV-absorbing material was observed when the anion-exchange column was eluted with 5 column volumes of 1.8 M (Et$_3$NH)(HCO$_3$) immediately following the purification gradient.

The extinction coefficient of *cis*-[Pt(NH$_3$)$_2$[d-(ApGpGpCpCpT)]] was determined to be $\epsilon_{260} \simeq 58\,200$ M^{-1} cm^{-1} per platinum (or per strand, vide infra), by a combination of atomic absorption and UV spectroscopic measurements. This value represents a 3.5% increase in ϵ_{260} over the value determined for the unmodified oligonucleotide.

Nuclear Magnetic Resonance Assignments. (i) Unplatinated Oligonucleotide. The [d(ApGpGpCpCpT)]$_2$ duplex contains a twofold symmetry rotation axis perpendicular to the helix axis at its midpoint, resulting in equivalent terminal (A·T), interior (G·C), and central (G·C) base pairs. The following schematic depicts the base numbering employed throughout this paper:

$$^{5'}\text{A(1)-p-G(2)-p-G(3)-p-C(4)-p-C(5)-p-T(6)}^{3'}$$

$$_{3'}\text{T(6)-p-C(5)-p-C(4)-p-G(3)-p-G(2)-p-A(1)}_{5'}$$

The 300-MHz ^{1}H NMR spectrum of nonexchangeable protons in the 8.5–1.5 ppm region of a 2.24 mM solution of [d-(ApGpGpCpCpT)]$_2$ in 100 mM phosphate buffer, pD 7.8, is presented in Figure 1. The nonexchangeable base protons occur in the downfield region of the spectrum, between 8.0 and 7.2 ppm. In Figure 1, the resonances numbered 1–4 are purine singlets, while resonances 5 and 7 are the cytosine H6 doublets (^3J = 7.4 Hz) and resonance 6 is the thymine H6 doublet, which appears as an unresolved quartet ($^4J \approx 1.3$ Hz). Upon prolonged heating to 93 °C in D_2O in the NMR probe, resonances 1, 3, and 4 decreased in intensity, characteristic of slowly exchanging purine H8 protons,[39] whereas resonance 2 remained unaffected and is therefore assigned as adenine(1) H2. The six H1′ resonances (resonances 8–12 and 14) and the two cytosine H5 doublets (resonances 13 and 15) are observed between 6.3 and 5.2 ppm. Selective-decoupling experiments indicated that doublets 5 and 13 are coupled to one another, as are doublets 7 and 15. The multiplet centered at 5.970 ppm (resonances 11 and 12) corresponds to an overlap of two H1′ protons.

The 2′-deoxyribose H3′ protons are found between 5.0 and 4.5 ppm (envelope 16), while H4′, H5′, and H5″ protons overlap extensively between 4.40 and 3.90 ppm (envelope 17). An exception is the pair of H5′, H5″ protons of adenine(1), which form a characteristic distorted AB doublet of doublets centered at 3.590 ppm (envelope 18).

The three resonance envelopes (resonances 19–21) and the lone multiplet (resonance 22) observed in the upfield region of the spectrum (2.80–1.60 ppm) arise from the six sets of H2′, H2″ protons of the 2′-deoxyribose moieties. Finally, the thymine methyl group (resonance 23) is located at 1.808 ppm (^4J = 1.3 Hz).

The deoxyribose protons were assigned by means of two-dimensional nuclear Overhauser effect (NOESY) and homonuclear chemical shift correlation (COSY) experiments. The proton resonances of each nucleotide residue were identified by means of NOE enhancements between the nonexchangeable base protons (purine H8, pyrimidine H6, H5) and their intranucleotide H1′, H2′, H3′ deoxyribose protons. Scalar coupling and intraresidue

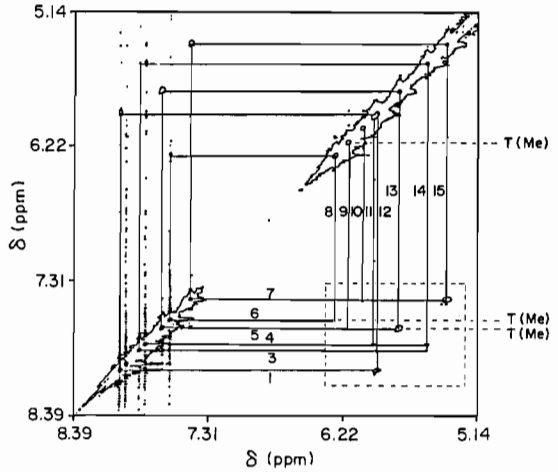

Figure 2. Contour map from NOESY spectrum of [d-(ApGpGpCpCpT)]$_2$ at 25 °C obtained with a mixing time of 275 ms. Sample conditions were the same as described in Figure 1. The spectrum shows the correlation peaks between the nonexchangeable base protons (resonances 1–7, 13, and 15; Figure 1) and the H1′ resonances (resonances 8–12 and 14, Figure 1). The one-dimensional spectrum appears along the diagonal.

(36) States, D. J.; Haberkorn, R. A.; Ruben, D. J. *J. Magn. Reson.* **1982**, *48*, 286–292.
(37) Fasman, G. D. In *Handbook of Biochemistry and Molecular Biology*, 3rd ed.; CRC: Cleveland, OH, 1975; Vol. I, p 589.
(38) Fichtinger-Schepman, A. M. J.; van der Veer, J. L.; Lohman, P. H. M.; Reedijk, J. *J. Inorg. Biochem.* **1984**, *21*, 103–112.
(39) Schweizer, M. P.; Chan, S. I.; Helmkamp, G. K.; T'so, P. O. P. *J. Am. Chem. Soc.* **1964**, *86*, 696–700.

Table I. ^{1}H Chemical Shifts (ppm) for [d{A(1)pG(2)pG(3)pC(4)pC(5)pT(6)}]$_2$[a]

	H8, H6	H3, H5, H2	H1′	H2″	H2′	H3′ (16)	H4′ (17)	H5′
adenine(1)	8.002 (1)	7.957 (2)	5.956 (12)	2.551	2.381	4.939	4.195	3.692 (18)
guanine (2)	7.845 (3)		5.583 (14)	2.737	2.695	4.990	4.375	4.091 (17)
guanine(3)	7.800 (4)		5.973 (11)	2.737	2.657	5.005	4.447	4.215 (17)
cytosine(4)	7.427 (7)	5.374 (15)	6.061 (10)	2.506	2.157	4.846	4.239	
cytosine(5)	7.666 (5)	5.762 (13)	6.173 (9)	2.518	2.345	4.867	4.254	
thymine(6)	7.592 (6)	1.738	6.278 (8)	2.525	2.338	4.584	4.122	

[a] Numbers in parentheses correspond to resonances identified in Figure 1.

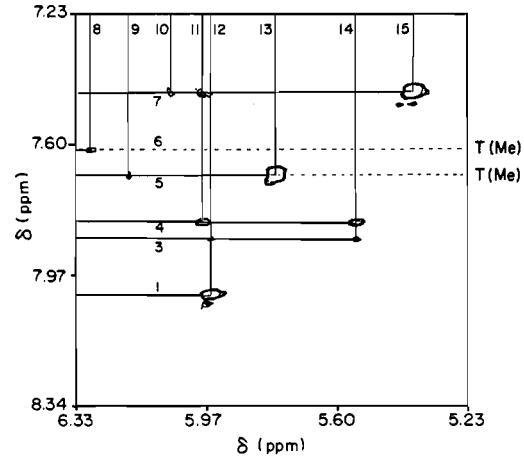

Figure 3. Expansion of the off-diagonal correlation peaks for the base–H1′ proton region enclosed by a dashed-line rectangle in Figure 2.

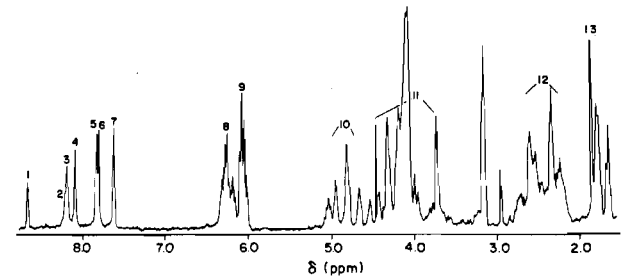

Figure 4. 300-MHz ^{1}H NMR spectrum of the nonexchangeable protons of 4.2 mM *cis*-[Pt(NH$_3$)$_2$[d(ApGpGpCpCpT)-*N7-G(2),N7-G(3)*]] in D_2O containing 100 mM potassium phosphate buffer, pD 7.8, at 45 °C. Adenine H8 (resonance 2) appears as a shoulder, while both cytosine H6 doublets overlap under these conditions. The 2′-deoxyribose H1′ resonances overlap extensively between 6.5 and 6.0 ppm. Resonance assignments are further identified in Table II.

NOE enhancements then allowed the complete assignment of each sugar spin system. Identification of the chain position of each nucleotide unit was determined by long-range NOE results between base$_{n-1}$–H1′$_n$ and base$_{n-1}$–H2″$_n$ protons. Redundancies in both the intrasugar and base–sugar connectivities allowed an internal consistency check on the assignments.[40]

Figures 2 and 3 display portions of a 2D NOE contour plot containing the NOE connectivities between the nonexchangeable base protons and the 2′-deoxyribose H1′ protons. These data were acquired by using a mixing time of 275 ms with presaturation of the HOD resonance under conditions that favored the duplex state of the oligonucleotide (25 °C, 100 mM phosphate buffer, pD 7.8 (vide infra)). For an idealized DNA double helix, the terminal 5′-base will be associated with only a single correlation peak to its own H1′ resonance. Furthermore, the H2 proton of adenine is located in the minor groove facing solvent and is not close enough to any 2′-deoxyribose protons to create an intramolecular NOE enhancement.

As is seen in Figure 2 and 3, only resonance 2 shows no correlation peak, verifying its assignment as adenine(1) H2. Resonance 1 has a single correlation peak to the H1′ multiplet 12 and is assigned to the terminal adenine residue. The next two guanine H8 protons show correlation peaks both to their own H1′ protons and to the H1′ protons of their 5′-neighboring residue.

The pyrimidine H6 resonances may similarly be used to identify their respective deoxyribose protons. Resonance 7 is assigned to the cytosine(4) H6 doublet, since it shows a correlation peak to the H1′ proton of guanine(3) at 5.973 ppm (resonance 11). The two additional peaks observed at 6.061 (resonance 10) and 5.374 ppm (resonance 15) correspond to the cytosine(4) H1′ proton and the adjacent cytosine H5 proton. This assignment implies that the doublet at 7.666 ppm (resonance 5) belongs to the cytosine(5) base, while the resonance at 7.592 ppm (resonance 6) must correspond to the thymine H6 proton. This argument allows the assignment of resonances 8 and 9 as the H1′ protons of thymine(6) and cytosine(5) residues, respectively. Figure 2 shows additional data to support these assignments. The thymine(6) methyl group (resonance 23, 1.783 ppm) shows two correlation peaks, an intense one to its neighboring intrabase thymine H6 proton (resonance 6) and to the H1′ resonance of the cytosine(5) residue (resonance 9). Thus, by working in from both 5′- and 3′-ends of the oligonucleotide using the unique bases as starting points, it is possible to verify the base sequence and assign the H1′ resonances.

The H2′, H2″ protons are more difficult to assign unambiguously, owing to their similar chemical shift values. For an idealized A- or B-DNA double helix, the intraresidue nonexchangeable base–H2′ proton distance is shorter than the base–H2″ proton distance by 1.2–1.3 Å. Conversely, the distance between the H1′ and H2″ protons is ~0.6 Å shorter than the H1′–H2′ distance. Since the intensity of the NOE-induced peaks is proportional to r^{-6}, the H2′ and H2″ protons were distinguished, owing to the stronger H1′–H2″ and base–H2′ NOE enhancements. These results were confirmed by COSY experiments, which gave identical H1′–H2′, H1′–H2″ intradeoxyribose correlations. In addition, many of the base$_{n-1}$–H2″$_n$ NOE interactions were observed and found to be consistent with the previous assignments (Table I).

The H3′ protons were identified from NOE enhancements created by the nonexchangeable base protons and by chemical shift correlation experiments. Adenine(1) H8 shows a correlation peak to the resonance at 4.939 ppm, while guanine(2) and guanine(3) H8 protons are assigned to the resonances at 4.990 and 5.005 ppm, respectively. The cytosine H6 doublets identify their respective H3′ protons as cytosine(4) (4.846 ppm) and cytosine(5) (4.867 ppm). Finally, the H3′ resonance of the thymine(6) residue is assigned to the proton at 4.584 ppm. This resonance is the only 3′-proton not affected by broad-band ^{31}P decoupling, suggestive of the 3′-terminal position.

The remaining H4′, H5′, and H5″ protons were assigned by a combination of NOE and scalar coupling correlation experiments. All experiments were modified to suppress the HOD signal, such that adjacent correlations could be more clearly observed. The H5′, H5″ resonances of the three pyrimidine bases could not be unambiguously identified, however. The terminal adenine residue lacks a phosphate group, and accordingly, its H5′, H5″ protons are farthest upfield, centered at 3.692 ppm. No distinction in chemical shifts was observed for the adenine and guanine H5′, H5″ protons under the resolution restrictions of the experiments. A summary of the chemical shifts for [d(ApGpGpCpCpT)]$_2$ is given in Table I.

(ii) Platinated Oligonucleotide. Figure 4 shows the 300-MHz ^{1}H NMR spectrum of the nonexchangeable protons (9.0–1.0 ppm)

(40) Hare, D. R.; Wemmer, D. E.; Chou, S.-H.; Drobny, G. *J. Mol. Biol.* **1983**, *171*, 319–336.

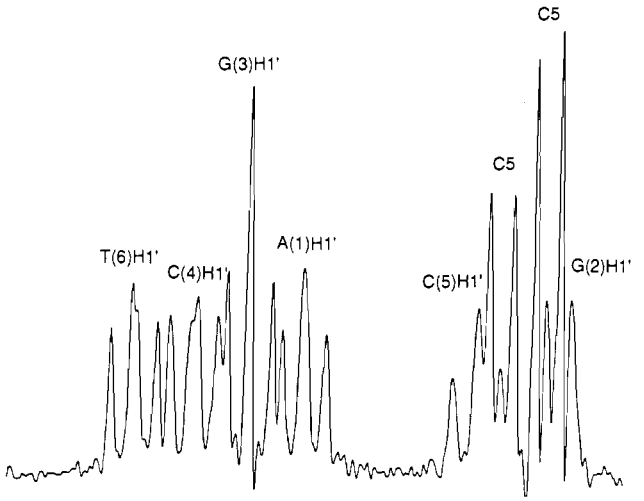

Figure 5. Expansion of and partial assignments in the 6.0–6.3 ppm region of the spectrum in Figure 4.

of *cis*-[Pt(NH$_3$)$_2$[d(ApGpGpCpCpT)]] (4.4 mM strand) in 100 mM phosphate buffer, pD 7.8, at 45 °C. The nonexchangeable base protons are located in the downfield region between 8.8 and 7.6 ppm. Resonances 1–4 are all singlets and correspond to the four purine base protons. Under these conditions, it was not possible to resolve resonance 2, which appears as a low-field shoulder on resonance 3. Only resonance 3 showed resistance to deuterium exchange and was therefore assigned as adenine(1) H2.

The three sets of pyrimidine resonances occur further upfield (7.9–7.6 ppm). Both cytosine H6 doublets (resonances 5 and 6) have coincidentally equal chemical shifts at 7.862 ppm under these conditions. The H6 proton of thymine(6) (resonance 7) is observed at 7.642 ppm and is coupled to the methyl group found upfield at 1.850 ppm (^4J = 1.3 Hz, resonance 13).

The next set of resonances (6.5–5.9 ppm, resonances 8 and 9) correspond to the six H1′ resonances of the 2′-deoxyribose rings and the two H5 doublets of cytosine(4) and cytosine(5) residues.

The six H3′ protons are observed further upfield (envelope 10), while the H4′, H5′, and H5″ protons overlap extensively between 4.5 and 3.8 ppm (envelope 11). Finally, the upfield region of the spectrum (2.8–1.6 ppm) contains the H2′, H2″ resonances, which cannot be resolved from their resonance envelopes (envelope 12).

The complete assignment of the resonances was obviated by the need for high temperature (55 °C) to prevent aggregation and sharpen the signals. These conditions, moreover, led to rapid exchange of the purine H8 resonances with deuterium from the solvent, causing a substantial decrease in the purine H8 signal intensities. Nonetheless, partial assignment of the resonances was made by identifying each 2′-deoxyribose spin system with the corresponding base by means of the NOE between the purine H8 or pyrimidine H6 protons and the H1′, H2′, or H3′ protons. Adenine(1) H2 (resonance 3) did not produce any intraresidue NOE enhancements, while the thymine(6) methyl group aided in the assignment of its own H1′ proton (6.291 ppm) and that of its 5′-neighboring base (cytosine(5), 6.092 ppm). The H1′ region of the *cis*-[Pt(NH$_3$)$_2$[d(ApGpGpCpCpT)]] spectrum (Figure 5) shows that four of the six H1′ multiplets appear within a 40-Hz region, while the remaining two H1′ resonances and the two cytosine H5 doublets appear in a 23-Hz region. A summary of assignments is given in Table II.

Identification of *cis*-[Pt(NH$_3$)$_2$Cl$_2$] Binding Site. Platinum(II) compounds bind covalently to heterocyclic nitrogen atoms of purine and pyrimidine bases.[5,6,24,41,42] This interaction decreases the pK_a values of ring imino nitrogen atoms, facilitating determination of the metal binding site by comparing the pH dependence of the base proton chemical shifts of the adduct with that of the unmodified oligonucleotide.[5-8]

Table II. Selected ^{1}H Chemical Shifts (ppm) for *cis*-Pt(NH$_3$)$_2$-Modified d(ApGpGpCpCpT)[a]

	H8, H6	H2, H5	H1′	H3′ (10)
adenine(1)	8.191 (2)	8.180 (3)	6.204 (9)	4.895
guanine(2)	8.168 (4)		6.064 (9)	5.138
guanine(3)	8.835 (1)		6.221 (8)	5.029
cytosine(4)	7.844 (6)	6.095 (9)	6.239 (8)	4.852
cytosine(5)	7.860 (5)	6.064 (9)	6.092 (9)	4.679
thymine(6)	7.639 (7)		6.291 (8)	4.530

[a] Numbers in parentheses correspond to numbered resonances in Figure 4.

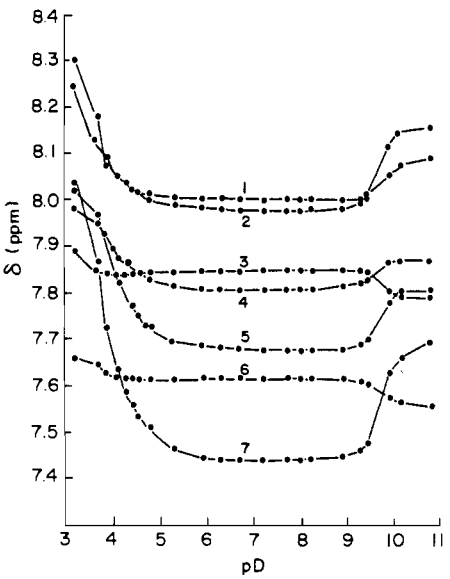

Figure 6. Chemical shift vs pD of the nonexchangeable base protons of [d(ApGpGpCpCpT)]$_2$. Resonance numbers correspond to those in Figure 1, and Table I lists the assignments.

The sigmoidal curves shown in Figure 6 reflect the effects of protonation or deprotonation of pyrimidine and purine ring nitrogen atoms of d(ApGpGpCpCpT).[43] In the low-pD range, the downfield shifts observed for the cytosine H6 doublets (pK_a 4.5: cytosine(5), 0.30 ppm; cytosine(4), 0.55 ppm), adenine(1) H8 and H2 (pK_a 3.7: 0.3 ppm), and guanine H8 (pK_a 2.3: guanine(2), 0.07 ppm; guanine(3), 0.17 ppm) are the result of the redistribution of π electron density in the heterocyclic ring system, owing to the removal of electron density by bound protons.

At high pD, deprotonations of guanine N1–H (pK_a 10.0) and thymine N3–H (pK_a 9.8) are observed. The upfield shifts of thymine(6) H6 (0.09 ppm) and guanine(2) H8 (0.12 ppm) are consistent with the introduction of additional negative charge into the ring system. The downfield shifts (0.15–0.35 ppm) of adenine(1) H8 and H2 and cytosine H6 resonances are a consequence of sequence-dependent nearest-neighbor base-stacking variations. Single-crystal X-ray and solution CD studies suggest that, while charged pyrimidines tend to destack, purines tend to stack but in a manner different from that of uncharged bases.[44] This decrease in base stacking results in less shielding, producing downfield shifts. The observed downfield shift of thymine(6) H6 at low pH and the unexpected downfield shift of guanine(3) H8 at high pH reflect the combined effects of base-stacking and protonation/deprotonation phenomena.

Figure 7 shows the pD dependence of the downfield resonances (9.0–7.5 ppm) of platinated d(ApGpGpCpCpT) over the pD range 3.4–9.0. No effect is observed at high pD for either cytosine H6

(41) Howe-Grant, M. E.; Lippard, S. J. *Met. Ions. Biol. Syst.* **1980**, *11*, 63–125.
(42) Girault, J.-P.; Chottard, J.-C.; Guittet, E. R.; Lallemand, J.-Y.; Huynh-Dinh, T.; Igolen, J. *Biochem. Biophys. Res. Commun.* **1982**, *109*, 1157–1163.
(43) Izatt, R. M.; Christensen, J. J.; Rytting, J. H. *Chem. Rev.* **1971**, *71*, 439–481.
(44) Saenger, W. In *Principles of Nucleic Acid Structure*; Springer-Verlag: New York, 1984.

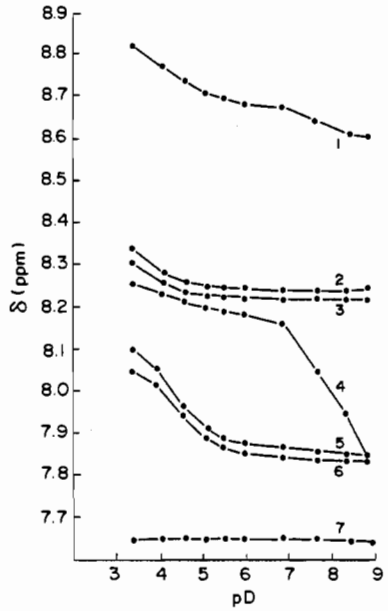

Figure 7. Chemical shift vs pD of the nonexchangeable base protons of *cis*-DDP-modified [d(ApGpGpCpCpT)]$_2$ at 70 °C. Resonance numbers correspond to those in Figure 5, and assignments are given in Table II.

doublet. At low pD, however, both cytosine resonances show characteristic shifts resulting from protonation at N3, the observed pK_a values of which agree well with those reported in the literature.[43] Throughout this range of pD values, the thymine(6) H6 resonance is invariant.

The pD dependence of the pyrimidine protons is characteristic of unmodified bases. Under conditions near neutral pD, the N3 position of thymine is protonated and is unavailable for metal binding. The lack of reactivity of *cis*-[Pt(NH$_3$)$_2$Cl$_2$] with thymine at neutral pH is well documented.[45] The observed titration of both cytosine bases at low pD values precludes their involvement in platinum binding. This conclusion is supported by the equivalent environments of the two bases, as evidenced by their chemical shifts.

A comparison of the pD profiles of the purine proton resonances of [d(ApGpGpCpCpT)]$_2$ and its *cis*-[Pt(NH$_3$)$_2$Cl$_2$]$_2$ adduct reveals significant differences in the pD range pD 5–9. While adenine(1) H8 and adenine(1) H2 exhibit pD-independent behavior, guanine(3) H8 (8.673 ppm) and guanine(2) H8 (8.151 ppm) shift upfield with increasing pD. Their observed pK_a values are ~8.0, indicating the removal of two imino protons from the two guanine moieties. A reduction in pK_a of the guanine N1 proton, from 10.0 in the oligonucleotide to 8.0 in its *cis*-DDP adduct, is characteristic of platinum(II) binding to guanine N7.[5-7,24,42] This phenomenon is also reported for *cis*-[Pt(NH$_3$)$_2$Cl$_2$] binding to mono- and dinucleotides.[5,6] Coordination to guanine N7 is also consistent with the downfield shifts (0.30–0.90 ppm) of the H8 resonances, owing to the inductive effect of platinum(II).[5-8]

The behavior of the adenine(1) H2 and H8 resonances over the pD range 3.4–5.0 argues against the possibility of an adenine(1) N7–guanine(2) N7 platinum adduct. If platinum were bound to adenine N7, the basicity of the N1 site would decrease by 1.5–2.0 pK_a units, shifting the titration below the range examined. The observed downfield shifts near pD 3.4 of adenine(1) H8 and H2 indicate protonation at the N1 site, thereby eliminating this possibility.

Anion-exchange chromatography results and the pD titration data rule out an interstrand guanine N7–guanine N7 cross-link. Not only would such an adduct have a charge of −8 but, in addition, only one guanine base per strand would show a depressed pK_a value. Figure 7 clearly indicates that both guanine residues have lowered pK_a values. The observation that *cis*-[Pt(NH$_3$)$_2$-{d(ApGpGpCpCpT)}] elutes as a trianion also rules out the possibility that two *cis*-{Pt(NH$_3$)$_2$}$^{2+}$ units form two interstrand guanine N7–guanine N7 cross-links (−6 net charge).

Table III. Imino Proton Resonances of [d(ApGpGpCpCpT)]$_2$ as a Function of Temperature

temp, °C	chem shift, ppm	$\Delta\nu_{1/2}$, Hz	temp, °C	chem shift, ppm	$\Delta\nu_{1/2}$, Hz
−12	12.95	36.4	8	13.02	19.7
−9	12.97	36.3	14	13.03	21.6
−5	13.01	27.6	20	13.02	32.5
−1	13.01	18.7	27	13.01	69.6
3	13.02	19.7	34	12.98	~120

The fact that both guanine H8 resonances exhibit depressed pK_a values argues against the proposed N7–O6 intrabase chelate. The possibility that two guanine N7–O6 chelates exist per strand is refuted by the net charge and the measured extinction coefficient per platinum. The presence of two platinum atoms per strand would result in an ϵ_{260} value of 116 400 per strand, a number well above the 5–15% increase typically induced by platinum binding.

The results presented above are consistent only with a nearest-neighbor *cis*-[Pt(NH$_3$)$_2$]{d(ApGpGpCpCpT)-*N7-G(2),N7-G(3)*}] intrastrand cross-link. This adduct is formed as the *only* significant product during the long-term reaction of *cis*-[Pt(NH$_3$)$_2$Cl$_2$] and [d(ApGpGpCpCpT)]$_2$. The type and number of adducts formed by *trans*-DDP are markedly different. Unlike the cis isomer, *trans*-DDP reacts with [d(ApGpGpCpCpT)]$_2$ to produce a distribution of species containing monofunctional G(2), G(3), and A(1) adducts, a *trans*-[Pt(NH$_3$)$_2$]{d(ApGpGpCpCpT-*N7-A(1),N7-G(3)*}] intrastrand cross-link, and significant amounts of highly charged interstrand cross-linked adducts.[22] This difference reflects the stereochemical requirements of the trans isomer which precludes formation of a nearest-neighbor type of cross-link.

Helix → Coil Transition of [d(ApGpGpCpCpT)]$_2$ and Its *cis*-[Pt(NH$_3$)$_2$Cl$_2$] Adduct. (i) Temperature-Dependence Studies of Exchangeable Protons. Tritium-exchange studies have determined the half-life for exchange with water of imino protons involved in Watson–Crick base-pair hydrogen bonding to be on the order of minutes.[46,47] This slow rate is in contrast to the rapid exchange of guanine N1–H and thymine N3–H protons of free mononucleotides in water, which occurs on the millisecond time scale.[48-50] Exchange of Watson–Crick base-paired protons is slow enough in the duplex state that they can be easily observed by ^{1}H NMR spectroscopy. When the duplex is disrupted, however, either by binding of small molecules or by thermal denaturation, the exchange rate of protons with solvent in the open form is fast enough to preclude observation.

The fact that exchangeable imino resonances appear in the proton NMR spectrum between 15 and 12 ppm for [d(ApGpGpCpCpT)]$_2$ in aqueous MeOH solutions clearly demonstrates the duplex nature of this oligonucleotide at low temperatures.[51,52] A single broad resonance centered at 12.95 ppm is observed in the region expected for G·C imino protons, while no A·T imino resonances occur at their expected lower field position (14.6 ± 1.0 ppm).[53-55] This result could arise either from an accidental equivalence of all three sets of imino protons or, more likely, from an equivalence of both G·C imino resonances coupled with fast exchange with solvent of the frayed A(1)·T(6) thymine N3–H imino protons. Equivalence of the imino protons of the [–GpGpCpC–]$_2$ core of [d(ApGpGpCpCpT)]$_2$ is consistent

(45) Mansy, S.; Chu, G. Y. H.; Duncan, R. E.; Tobias, R. S. *J. Am. Chem. Soc.* **1978**, *100*, 607–616.
(46) Teitelbaum, H.; Englander, S. W. *J. Mol. Biol.* **1975**, *92*, 55–78.
(47) Teitelbaum, H.; Englander, S. W. *J. Mol. Biol.* **1975**, *92*, 79–92.
(48) Crothers, D. M.; Hilbers, C. W.; Shulman, R. G. *Proc. Natl. Acad. Sci. U.S.A.* **1973**, *70*, 2899–2901.
(49) Englander, J. J.; Kallenbach, N. R.; Englander, S. W. *J. Mol. Biol.* **1972**, *63*, 153–169.
(50) Englander, J. J.; von Hippel, P. H. *J. Mol. Biol.* **1972**, *63*, 171–177.
(51) Patel, D. J. *Biopolymers* **1976**, *15*, 533–558.
(52) Patel, D. J. *Biopolymers* **1977**, *16*, 1635–1656.
(53) Kearns, D. R.; Patel, D. J.; Shulman, R. G. *Nature (London)* **1971**, *229*, 338–339.
(54) Patel, D. J.; Tonelli, A. E. *Biopolymers* **1974**, *13*, 1943–1964.
(55) Patel, D. J.; Tonelli, A. E. *Proc. Natl. Acad. Sci. U.S.A.* **1974**, *71*, 1945–1948.

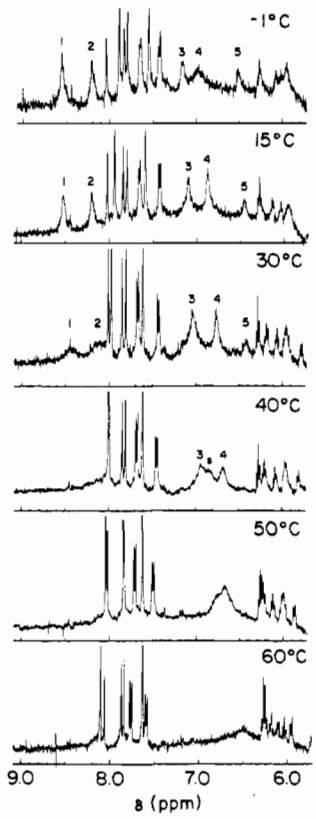

Figure 8. Temperature dependence of selected 360-MHz ^{1}H NMR spectra (amino resonances) of $[d(ApGpGpCpCpT)]_2$ (2.24 mM duplex concentration) in 3/2 v/v water (90% H_2O, 10% D_2O)/MeOH containing 100 mM potassium phosphate buffer, pH 7.4.

with results reported for $[d(GpGpCpC)]_2$ and $[d(CpCpGpG)]_2$.[52] In both instances, a single resonance was observed at 13.1 and 13.4 ppm, respectively, which slowly broadened out as the temperature increased. This behavior is in contrast to the report of two imino resonances at 0 °C for $[d(TpGpGpCpCpA)]_2$ (13.22 and 13.15 ppm).[56] The downfield resonance broadened out at 10 °C (assigned to G(2)·C(5)), whereas the resonance at 13.15 ppm vanished at approximately 22 °C (assigned to G(3)·C(4)). The existence of two G·C imino protons for $[d(TpGpGpCpCpA)]_2$ and only one for $[d(ApGpGpCpCpT)]_2$ may arise from greater shielding effects of a 5′-neighboring purine base (adenine) relative to that of a pyrimidine base (thymine). Since the chemical shift of an isolated G·C imino resonance is reported as 13.75 ppm,[54,55] any purine → pyrimidine change in sequence would increase the observed resonance frequency of a 3′-neighboring imino proton.

Table III contains the chemical shift and $\Delta\nu_{1/2}$ values of the $[d(ApGpGpCpCpT)]_2$ imino resonances as a function of temperature from −12 to +34 °C. The resonances do not shift upfield as a function of temperature. Instead, they exhibit temperature-independent behavior and appear to sharpen between −12 and +8 °C (36.4–19.7 Hz) before broadening and vanishing at 34 °C. Since all nonexchangeable base protons are sharp at −10 °C, the possibility that broadening is due to an increase in solvent viscosity is excluded. Instead, the results are most likely due to exchange of the G(2)·C(5) imino protons with H_2O between −12 and +8 °C, leaving only the G(3)·C(4) imino resonances to exchange at higher temperature (34 °C). Overlap of the two sets of imino resonances precluded the possibility of obtaining accurate dissociation or exchange rates for the individual base pairs.

The amino resonances involved in duplex hydrogen bonding occur further upfield than the imino resonances, typically falling between 8.5 and 5.5 ppm[52] (Figure 8). As a consequence of the partial cytosine C4–NH_2 double-bond character, two amino resonances will be observed.[57-61] Studies with mono- and dinucleotides demonstrated that the amino proton involved in base-pair hydrogen bonding resonates at lower field than the proton facing solvent. This behavior is in contrast to that of the guanine amino group, which rotates rapidly on the NMR time scale, so that only an averaged resonance for the two protons can be observed, even at low temperatures.[60,61]

Although the G(2)·C(5) and G(3)·C(4) imino resonances are accidentally equivalent, two sets of cytosine amino protons and two time-averaged guanine amino resonances are seen at low temperature. The temperature dependence of these protons is shown in Figure 8.

The resonances at 8.542 and 8.202 ppm (resonances 1 and 2, −1 °C, Figure 8) are assigned to the cytosine amino protons involved in hydrogen bonding to the O6 keto groups of the two guanine bases. Saturation-transfer experiments carried out at 7 °C identified the protons of the individual amino groups (resonances 1 and 3, 7.121 ppm; resonances 2 and 5, 6.474 ppm). These studies indicate that, at 7 °C, resonance 3 corresponds to the accidental overlap of a cytosine amino proton and the protons of a guanine amino group (Figure 8, higher temperatures). Although the internal and central cytosine amino protons are well resolved, both sets of resonances exhibit identical temperature-dependent behavior, precluding their assignment.

The two additional exchangeable resonances observed at 7.133 and 6.977 ppm (resonances 3 and 4) are assigned as the time-averaged guanine NH_2 protons. No assignments can be made despite their different chemical shifts, owing to their similar behavior with temperature.

Line widths of the cytosine and guanine amino resonances show distinctly different temperature-dependent behavior. Whereas the cytosine resonances broaden with increasing temperature (−1 to +25 °C), the guanine resonances sharpen. This result suggests that, while rotation about the cytosine C4–NH_2 bond is slow at low temperatures (with respect to a 1.4 ppm difference in chemical shift) and increases to an intermediate rate near 25–30 °C, rotation about the guanine G2–NH_2 bond is intermediate at low temperature and increases as the temperature is raised. These results are consistent with CNDO/2 calculations, which predict a rotation barrier of 15–25 kcal/mol for cytosine[62,63] and 8–10 kcal/mol for guanine amino groups.[64]

At 35 °C, the cytosine amino resonances have vanished, while the guanine resonances remain quite intense. A shoulder can be observed on the high-field side of resonance 3, however, which becomes a distinct resonance at 40 °C (Figure 8). Although tentative, its assignment is consistent with the time-averaged temperature-shifted cytosine amino protons under conditions of fast rotation about the C4–NH_2 bond and duplex melting. As the temperature is increased, the remaining resonances broaden and shift upfield, eventually exchanging out near 65 °C.

These results are analogous to the general trends reported for $[d(CpCpGpG)]_2$, $[d(GpGpCpC)]_2$[51] and $[d(CpGpCpG)]_2$[52] in aqueous solution. The lower melting temperature of these oligonucleotides, however, prevented the observation of the rapid rotation of the cytosine amino group and, in the case of $[d(GpGpCpC)]_2$, the full set of amino resonances.

The distinction between fraying at the ends of an oligonucleotide and differential melting of the ends is worthy of comment.[65] By definition, a melted base pair is no longer involved in interstrand

(56) Guittet, E. R.; Pireteau, D.; Lallemand, J.-Y.; Huynh-Dinh, T.; Igolen, J. *Nucleic Acids Res.* **1984**, *12*, 5927–5941.
(57) Pullman, A.; Pullman, B. *Adv. Quantum Chem.* **1968**, *4*, 267–325.
(58) Raszka, M.; Kaplan, N. O. *Proc. Natl. Acad. Sci. U.S.A.* **1972**, *69*, 2025–2029.
(59) Shoup, R. R.; Miles, H. T.; Becker, E. D. *J. Phys. Chem.* **1972**, *76*, 64–70.
(60) McConnell, B.; Seawell, P. C. *Biochemistry* **1973**, *12*, 4426–4434.
(61) Krugh, T. R.; Laing, J. W.; Young, M. A. *Biochemistry* **1976**, *15*, 1224–1228.
(62) Geller, M.; Lesyng, B. *Biochim. Biophys. Acta* **1975**, *407*, 407–419.
(63) Rao, C. N. R. *Jerus. Symp. Quantum Chem. Biochem.* **1973**, *5*, 107–119.
(64) Rao, K. G.; Rao, C. N. R. *J. Chem. Soc., Perkin Trans. 2* **1973**, 889–891.
(65) Pardi, A.; Martin, F. N.; Tinoco, I., Jr. *Biochemistry* **1981**, *20*, 3986–3996.

Table IV. Thermodynamic Parameters Obtained from Temperature-Dependent Chemical Shift Studies

	T_M, °C[a]		T_M, °C[a]
adenine(1) H8	*b*	cytosine(4) H5	60.0
adenine(1) H2	51.0	cytosine(5) H6	62.0
guanine(2) H8	57.0	cytosine(5) H5	54.0
guanine(3) H8	60.0	thymine(6) H6	34.0
cytosine(4) H6	62.5	thymine(6) Me	39.0

[a] ±3 °C. [b] Could not be measured owing to its irregular behavior with temperature over the range $2 < T < 30$ °C.

hydrogen bonding or base pairing. At the terminal-base-pair T_M value (vide infra), there are equal concentrations of oligonucleotides with the terminal base pair intact and melted. Melting is an equilibrium phenomenon and depends solely on the concentrations of species in the two states. Fraying refers to a kinetic phenomenon and is defined as the rapid opening and closing of a particular base pair, described by the appropriate forward (opening) and reverse (closing) rate constants. The G(2)·C(5) and G(3)·C(4) imino resonances are observable at low temperatures but vanish near 34 °C, a temperature well below the T_M value of 60.0 ± 3.0 °C of the oligonucleotide (vide infra). This lack of observable imino resonances does not reflect the equilibrium concentrations of duplex and coil forms; the oligonucleotide is frayed but not melted. Studies of the nonexchangeable base protons of the [–GpGpCpC–]$_2$ core indicate that >95% of the oligonucleotide is duplex at 37 °C, a temperature at which no imino resonances are observed.

Finally, there are several possible explanations for the observed line broadening of the imino resonances without an accompanying upfield shift. One possibility is that exchange of the proton from the coil state with water occurs prior to return to the helix structure, such that the lifetime in the helix is limited by the exchange rate of the proton with solvent. Another is that fast exchange may be occurring between the helix and coil states, such that the average is weighted toward the side of the helix, precluding any observation of a chemical shift change. At present, these possibilities cannot be distinguished.

The spectrum of *cis*-[Pt(NH$_3$)$_2$[d(ApGpGpCpCpT)]] was recorded at 2 °C in 90% H$_2$O, 10% D$_2$O, 100 mM phosphate buffer, pH 7.4, by using the time-shared long-pulse solvent suppression sequence. Under no conditions were imino and amino resonances observed in the 15–10 and 9–5 ppm regions, respectively. This result was also observed for the *trans*-[Pt(NH$_3$)$_2$[d(ApGpGpCpCpT-*N7-A(1),N7-G(3)*)]] adduct of d(ApGpGpCpCpT), implying that, in each case, the platinated oligonucleotide adopts a single-stranded structure.[22] Any introduction of unmodified oligonucleotide resulted in solutions containing [d(ApGpGpCpCpT)]$_2$ and platinated single-stranded adducts.

(ii) Temperature-Dependence Studies of Nonexchangeable Protons. Proton NMR studies of the helix ⇌ coil transition for several oligonucleotides have demonstrated that differential melting values (T_M) for individual base pairs increase in the order terminal < internal < central.[51,52] In the present case, individual T_M values were determined by monitoring the chemical shift of each nonexchangeable base and H1′ proton as a function of temperature (2–93 °C, Figures 9 and 10). The remaining 2′-deoxyribose proton resonances could not be monitored, owing to extensive overlap. These data are summarized in Table IV.

The purine base resonances typically exhibit downfield shifts with increasing temperature, except for guanine(2) H8, which showed a slight upfield shift. Adenine(1) H8 and H2 resonances have significant temperature-dependent shifts over the range 2–30 °C, behavior expected for a terminal base, whereas guanine(3) H8 is virtually temperature-independent over the same range before shifting downfield by 0.11 ppm.

The thymine(6) H6 resonance exhibits a downfield shift of 0.07 ppm (7.551 to 7.624 ppm) over the range 2–45 °C, characteristic of its 3′-terminal position in the polymer. Similar low-temperature behavior is observed for the thymine methyl resonance. As depicted in Figure 9, the remaining two pyrimidine H6 doublet

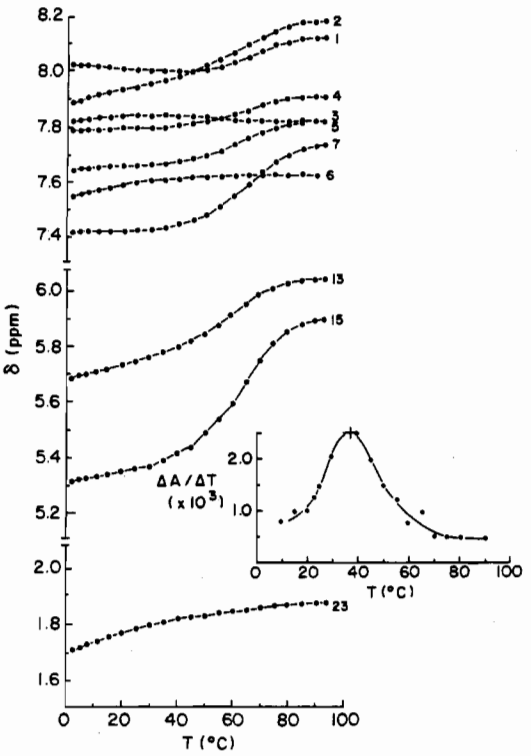

Figure 9. Chemical shift vs temperature of the aromatic purine (adenine H8, H2; guanine H8) and pyrimidine (cytosine H6, H5; thymine H6, methyl) protons in D$_2$O containing 100 mM potassium phosphate buffer at pD 7.8. Numbers alongside curves represent resonance numbers from Figure 1; assignments appear in Table I. The inset shows a plot of $d(A_{260})/dT$ obtained from temperature-dependent UV-absorption studies of [d(ApGpGpCpCpT)]$_2$ in 100 mM potassium phosphate buffer and D$_2$O at pD 7.8.

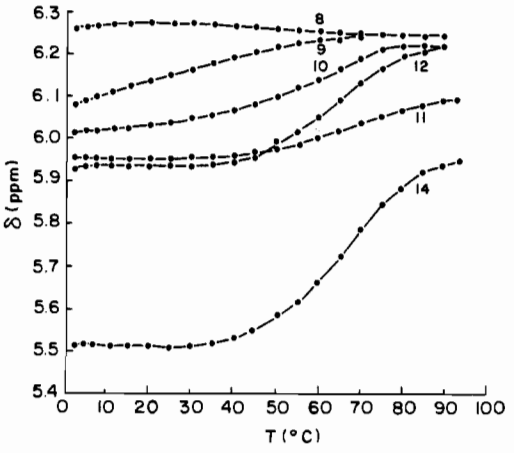

Figure 10. Chemical shift vs temperature of the six 2′-deoxyribose H1′ protons in D$_2$O containing 100 mM potassium phosphate buffer at pD 7.8. Numbers alongside temperature curves represent resonance assignments from Figure 1; assignments are given in Table I.

chemical shifts are invariant throughout the temperature range 2–35 °C before shifting downfield by 0.18 (cytosine(5)) and 0.31 ppm (cytosine(4)). This behavior is in contrast to that of both cytosine H5 doublets, which exhibit immediate and substantial downfield shifts (0.36 ppm, cytosine(5); 0.58 ppm, cytosine(4)) with increasing temperature.

All H1′ protons become more shielded as the temperature is lowered from 93 to 2 °C, except for the thymine(6) H1′ multiplet at 6.173 ppm. This resonance shows an anomalous downfield shift of 0.03 ppm between 93 and 25 °C before moving to higher fields. Typically, chemical shift differences of 0.15–0.40 ppm were observed between 93 and 2 °C. As is evident from Figure 10, the six H1′ resonances may be divided into two sets on the basis of their temperature-dependent chemical shifts over the range 2–35

°C. The first set consists of the pyrimidine H1′ multiplets, which show temperature-dependent shifts, while the second set, containing the three purine H1′ multiplets, have temperature-invariant chemical shifts. This difference is thought to reflect the relative base-stacking interactions (purine·purine > purine·pyrimidine > pyrimidine·pyrimidine).[44]

The temperature-dependence studies were also performed in 5 mM phosphate buffer, pD 7.8. Although the overall features under these conditions are identical with those described above for 100 mM phosphate buffer, a decrease in the midpoint of the melting profiles of approximately 5 °C for each of the nonexchangeable base protons is observed, a consequence of the decrease in duplex stability owing to the reduction in ionic strength.[44]

The temperature dependence of the chemical shifts of the observable base resonances was reversible, as verified through a heating, cooling, and reheating cycle. In all cases, the resonances fell on the melting curves in reproducible fashion, indicating complete reversibility of the melting transitions.

The data in Table IV reveal that the terminal A(1)·T(6) base pair of $[d(ApGpGpCpCpT)]_2$ has a T_M value 10–15 °C lower than the average T_M value of the $[-GpGpCpC-]_2$ core (43.0 ± 9.0 and 60.0 ± 3.0 °C, respectively). This difference suggests that, below 40 °C, the A(1)·T(6) base pair is largely intact (but frayed) whereas, above 50 °C, only the $[-GpGpCpC-]_2$ core is in the duplex state. A narrow range of T_M values (60 ± 3 °C) is observed for the central four base pairs (excluding pyrimidine H(5) resonances[52]), G(2)·C(5) and G(3)·C(4), indicating that they melt simultaneously.

Additional evidence supporting the noncooperative melting of $[d(ApGpGpCpCpT)]_2$ comes from temperature-dependent UV-absorption studies (Figure 9, inset). An 11% increase in hyperchromicity occurs uniformly over a temperature range of 70 °C (15–85 °C), indicating a sequential melting process.

This result is contrary to the report of cooperative melting for $[d(TpGpGpCpCpA)]_2$ (3 mM strand, T_M 40 °C), where nearly equivalent T_M values for all base pairs were reported.[56] Calculated stabilities of nearest-neighbor base-pair doublets indicate that a d(TpG)·d(ApC) dimer is comparable in stability to a d(ApG)·d(TpC) dimer,[66] precluding the possibility that sequence-dependent base-stacking interactions would cause different terminal T_M values.

The stabilizing influence of the terminal A(1)·T(6) base pair is most clearly demonstrated by comparing the T_M value of the central four base pairs in $[d(ApGpGpCpCpT)]_2$ (60.0 ± 3.0 °C) with those of $[d(CpCpGpG)]_2$ (20.0 mM strand, 38 °C), $[d(GpGpCpC)]_2$ (20.0 mM strand, 42 °C),[52] and $[d(CpGpCpG)]_2$ (4.7 mM strand, 50 °C).[51] All values were obtained in either 100 mM phosphate or 100 mM cacodylate buffer. The increased stability resulting from a G·C-rich core is evident by noting the T_M values of $[d(ApTpGpCpApT)]_2$ (14 mM strand, 35 °C),[67] $[d(GpGpApApTpTpCpC)]_2$ (5.3 mM strand, 46 °C),[68] and $[d(CpGpCpGpCpG)]_2$ (4.8 mM strand, 67 °C).[51] Differences in T_M values of duplex oligonucleotides depend on many factors, among which are nearest-neighbor base-stacking interactions. The stabilities of the 10 types of nearest-neighbor base-pair doublets have been calculated and increase in the order d(ApG)·d(TpC) ≪ d(GpG)·d(CpC) ≪ d(GpC)·d(CpG).[69] This result suggests that the difference between the T_M values of $[d(ApGpGpCpCpT)]_2$ and $[d(ApTpGpCpApT)]_2$ or $[d(GpGpApApTpTpCpC)]_2$ is due to the position and number of the less stable A·T base pairs.

This analysis does not explain the large discrepancy in T_M values obtained for $[d(ApGpGpCpCpT)]_2$ and $[d(TpGpGpCpCpA)]_2$,[56] however. The difference of 20 °C between T_M values of these closely related oligonucleotides is not presently understood. Although part of this difference may result from ionic strength variations, no buffer concentration having been reported for $[d(TpGpGpCpCpA)]_2$, the magnitude of the effect is unexpected.

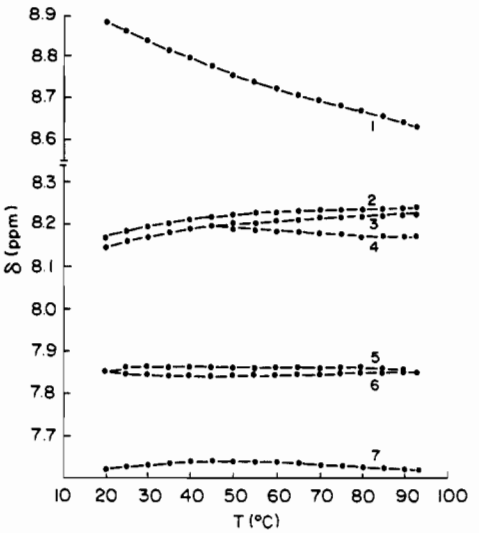

Figure 11. Chemical shift vs temperature of the nonexchangeable base protons of *cis*-DDP-modified $[d(ApGpGpCpCpT)]_2$ in D_2O containing 100 mM potassium phosphate buffer at pD 7.8. Numbers alongside temperature curves represent resonance assignments from Figure 5, and assignments are given in Table II.

The inset of Figure 9 shows the midpoint of the melting transition determined by UV-absorption spectroscopy (100 mM potassium phosphate, pD 7.8, T_M = 37.0 ± 2.0 °C) to be substantially lower than the T_M value obtained through ^1H NMR analysis (60.0 ± 3.0 °C). This difference (23 °C) arises from the different concentrations of oligonucleotide used in the optical studies (15.9 μM strand) and NMR experiments (4.48 mM strand). Similar results were reported for the melting of $[r(ApApGpCpUpU)]_2$, where a maximum difference of 29 °C was observed between the optical T_M value (21 °C, 10 μM strand) and the ^1H NMR T_M value (50 °C, 10 mM strand).[70]

Figure 11 shows the temperature-dependent chemical shifts (20–93 °C) of the nonexchangeable base protons of *cis*-$[Pt(NH_3)_2\{d(ApGpGpCpCpT)\}]$ in 100 mM phosphate buffer, 1 mM Na_2EDTA, pD 7.8. These resonances experience severe line broadening below 35 °C, indicating aggregation or dynamic conformational change phenomena. The downfield guanine(3) H8 (resonance 1) is particularly sensitive to temperature, exhibiting line widths of 20 Hz near 20 °C. Owing to excessive line broadening, no data were collected below 20 °C. As a consequence of the extensive overlapping of resonances, the deoxyribose and cytosine H5 protons could not be monitored.

The four purine resonances (resonances 1–4) demonstrate two types of temperature-dependent behavior. The guanine(3) H8 proton (8.774 ppm) is very sensitive to temperature, continuously shifting upfield by 0.3 ppm between 20 and 93 °C (8.886 ppm, 20 °C; 8.637 ppm, 93 °C). The direction of this shift was unexpected from simple base-destacking arguments. The remaining three purine resonances show only slight temperature dependencies, less than a 0.08 ppm shift over the same range (adenine(1) H2, 0.07 ppm; adenine(1) H8, 0.08 ppm; guanine(2) H8, 0.03 ppm). The pyrimidine resonances were virtually temperature-independent over the entire range studied.

Phosphodiester ^{31}P NMR Resonances. The ^{31}P NMR resonances of $[d(ApGpGpCpCpT)]_2$ show significant downfield shifts beginning at 25 °C and continuing through 90 °C (Figure 12). Theoretical and experimental evidence suggests that a primary difference occurs in the geometry of the internucleotide phosphodiester bonds[71–73] between base-stacked and coil structures.

(66) Gotoh, O.; Tagashira, Y. *Biopolymers* **1981**, *20*, 1033–1042.
(67) Patel, D. J. *Biochemistry* **1975**, *14*, 3984–3989.
(68) Patel, D. J.; Canuel, L. L. *Eur. J. Biochem.* **1979**, *96*, 267–276.
(69) Ornstein, R. L.; Rein, R.; Breen, D. L.; MacElroy, R. D. *Biopolymers* **1978**, *17*, 2341–2360.
(70) Borer, P. N.; Kan, L. S.; T'so, P. O. P. *Biochemistry* **1975**, *14*, 4847–4863.
(71) Olson, W. K. *Biopolymers* **1975**, *14*, 1797–1810.
(72) Yathindra, N.; Sundaralingam, M. *Proc. Natl. Acad. Sci. U.S.A.* **1974**, *71*, 3325–3328.

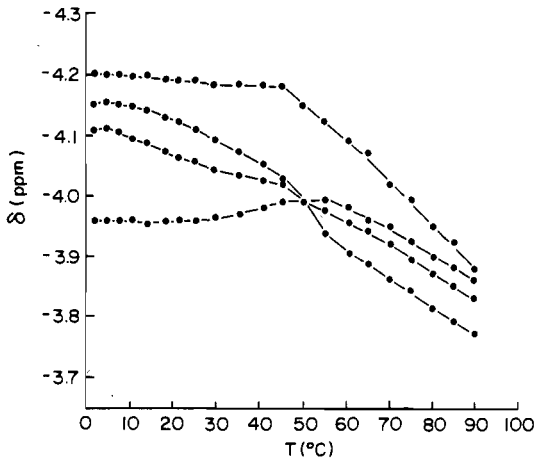

Figure 12. Temperature dependence of the ^{31}P NMR chemical shifts of [d(ApGpGpCpCpT)]$_2$ (10.17 mM duplex concentrations) in D_2O containing 100 mM potassium phosphate buffer at pD 7.8.

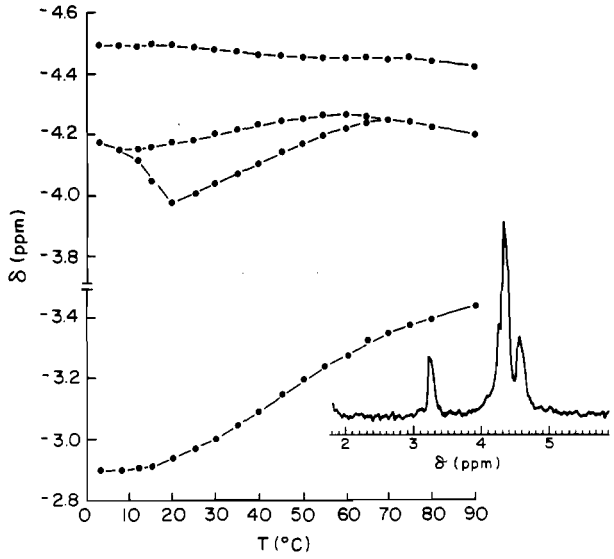

Figure 13. Temperature dependence of the ^{31}P NMR chemical shifts of *cis*-DDP-modified [d(ApGpGpCpCpT)]$_2$ in D_2O containing 100 mM potassium phosphate buffer at pD 7.8. The inset shows the 202-MHz ^{31}P NMR spectrum of *cis*-[Pt(NH$_3$)$_2$]{d(ApGpGpCpCpT)-*N7-G(2),N7-G(3)*}] obtained at 60 °C. The lone resonance at 3.283 ppm is assigned as the phosphodiester group linking the two coordinated guanine nucleosides (see text).

The α and ζ torsion angles, O3′–P–O5′–C5′ and C3′–O3′–P–O5′, respectively, typically found in the gauche–gauche (gg) conformation in helical structures, change to gauche–trans (gt) configuration in the coil state, resulting in a lengthening of the interphosphate distance. Therefore, whereas nonexchangeable base proton resonances are useful monitors of base-stacking interactions, ^{31}P resonances largely reflect variations in the O–P–O backbone.

The four ^{31}P NMR resonances observed at low temperature reveal that a distribution of gg conformations exists. As shown in Figure 12, two resonances are temperature-dependent below 35 °C. Above this temperature, each resonance shifts 0.2–0.35 ppm downfield, indicative of gg → gt transitions. Even at 90 °C, four distinct resonances are observed. On the basis of current information, no unambiguous assignments of the ^{31}P NMR resonances can be made.

Figure 13 depicts the ^{31}P NMR chemical shifts of the five phosphate groups of *cis*-[Pt(NH$_3$)$_2$]{d(ApGpGpCpCpT)}] plotted as a function of temperature (3–93 °C). The inset of Figure 13 shows that four of the resonances occur within a chemical shift range of 0.5 ppm. Immediately obvious is a lone downfield resonance, separated from the remaining ^{31}P resonances by 0.8–1.4 ppm. While the chemical shifts of the upfield ^{31}P resonances are nearly temperature-independent, the resonance at −3.02 ppm (30 °C) shifts upfield by 0.45 ppm with increasing temperature. Selective ^{31}P NMR decoupling experiments (Figure 14) allowed the assignment of this resonance as the phosphate group between the two guanosine residues. Similar assignments have been made for *cis*-[Pt(NH$_3$)$_2$]{d(TpCpTpCpGpGpTpCpTpC)}],[11] [Pt(en){d(GpGpApApTpTpCpC)}],[74] [Pt(en){d(ApTpTpGpGpTpTpApApCpCpApApT)}],[74] *cis*-[Pt(NH$_3$)$_2$]{d(TpApTpApTpGpGpCpCpApTpApTpA)}],[74] and [Pt(en){d(ApTpApTpGpGpTpApCpCpApTpApT)}].[74] The chemical shift at the highest temperature, −3.45 ppm at 90 °C, is similar to the room-temperature ^{31}P NMR shifts of *cis*-[Pt(NH$_3$)$_2$]{d(GpG)}],[9] [Pt(en){d(GpGpTpT)}],[74] and [Pt(en){d(GpGpApApTpTpCpC)}].[74] These complexes have no flanking nucleotide or phosphate group 5′ to the d(GpG) unit. The low-temperature shift (−2.90 ppm, 3 °C) is analogous to that reported for *cis*-[Pt(NH$_3$)$_2$]{d(CpGpG)}][14] (−2.50 ppm, 5 °C), which also moves upfield with increasing temperature. It is proposed that a combination of base-stacking interactions and hydrogen bonding between the 5′-phosphate of the pGpG moiety and the ammine ligands of the *cis*-{Pt(NH$_3$)$_2$}$^{2+}$ unit[74,75] is responsible for the downfield shift of this resonance.[11,74,75] Both molecular mechanics calculations on *cis*-[Pt(NH$_3$)$_2$]{d(GpGpCpCpG*pG*pCpC)}]·d-

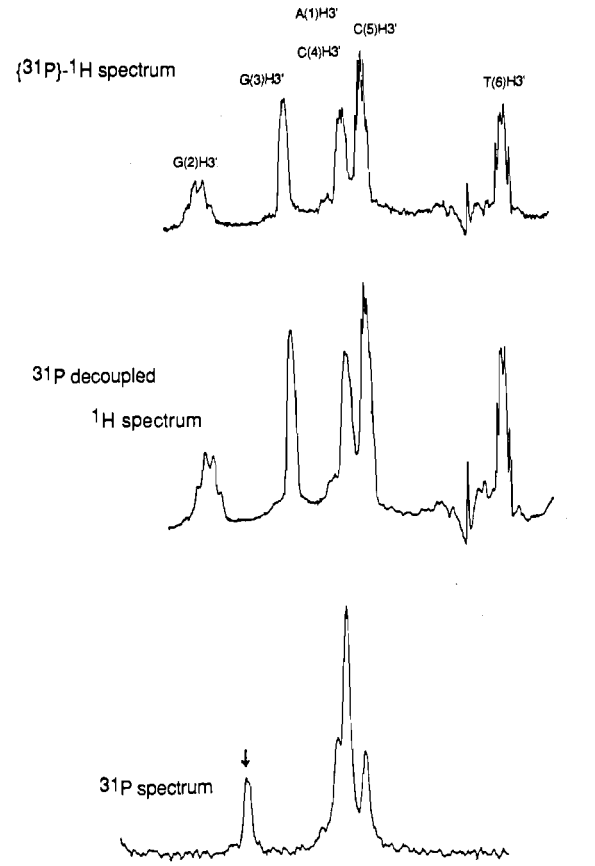

Figure 14. Selective ^{1}H{^{31}P} NMR experiments of *cis*-DDP-modified [d(ApGpGpCpCpT)]$_2$ in D_2O containing 100 mM potassium phosphate buffer at pD 7.8. The top trace corresponds to the broad-band ^{1}H{^{31}P} spectrum of the H3′ region. The middle trace depicts the H3′ proton spectral region in which the lone resonance at 3.15 ppm of the ^{31}P NMR spectrum (bottom trace) was selectively decoupled.

(73) Calascibetta, F. G.; Dentini, M.; DeSantis, P.; Moresetti, S. *Biopolymers* **1975**, *14*, 1667–1684.

(74) (a) Marzilli, L. G.; Reily, M. D.; Heyl, B. L.; McMurray, C. T.; Wilson, W. D. *FEBS Lett.* **1984**, *176*, 389–392. (b) Fouts, C. S.; Reily, M. D.; Marzilli, L. G.; Zon, G. *Inorg. Chim. Acta* **1987**, *137*, 1–13.

(75) (a) Reily, M. D.; Marzilli, L. G. *J. Am. Chem. Soc.* **1985**, *107*, 4916–4924. (b) Byrd, R. A.; Summers, M. F.; Zon, G.; Fouts, C. S.; Marzilli, L. G. *J. Am. Chem. Soc.* **1986**, *108*, 504–505.

(GpGpCpCpGpGpCpC)[15] and *cis*-[Pt(NH$_3$)$_2$\{d-(TpCpTpCpG*pG*pTpCpTpC)\}]·d(GpApGpApCpCpGpAp-GpA)[15,16] and the X-ray crystal structures of *cis*-[Pt(NH$_3$)$_2$\{d-(pGpG)\}][13] and *cis*-[Pt(NH$_3$)$_2$\{d(CpG*pG*)\}][14] have shown the existence of this type of hydrogen bonding. The component of the total ^{31}P NMR chemical shift arising from these interactions should decrease with increasing temperature, resulting in an upfield shift of the resonance. At present, a more definitive explanation for this chemical shift cannot be given.

Lack of any significant temperature-dependent behavior of the remaining ^{31}P resonances in *cis*-[Pt(NH$_3$)$_2$\{d(ApGpGpCpCpT)\}] attests to the single-stranded nature of the adduct.

Conformation of [d(ApGpGpCpCpT)]$_2$. (i) Glycosidic Bond Torsion Angles. For a regular Watson–Crick double helix with right-handed antiparallel strands, the bases adopt an anti configuration about the glycosidic bond.[44] Adenine H2 protons point toward the interior of the duplex, away from nearby nonexchangeable protons, while purine H8 and pyrimidine H6 protons are near the H2′, H3′, and H5′ deoxyribose ring protons. Accordingly, T_1 for adenine(1) H2 (2.96 s) is substantially longer than the values of the purine H8 (adenine(1) H8, 1.16 s; guanine(2) H8, 0.96 s; guanine(3) H8, 0.95 s) or pyrimidine H6 (cytosine(4), 0.85 s; cytosine(5), 0.77 s; thymine(6), 0.89 s) protons. Additional evidence for anti base conformations is provided by the T_1(purine H8)/T_1(H1′) ratios,[76] which depend on the rotational angle about the glycosidic bond, providing a qualitative measure of the syn/anti orientation. Values of ~0.5 or ~1.5 indicate anti or syn conformations, respectively. The three ratios (r) measured at 30 °C (adenine(1), r = 0.80; guanine(2), r = 0.72; guanine(3), r = 0.70) are consistent with anti geometry for each purine base. This assignment is supported by 2D NOE experiments, revealing strong purine H8 to H3′ and H2′ and pyrimidine H6 to H3′ and H2′ NOE enhancements.

(ii) Deoxyribose Ring Geometry. Torsion angles (Φ) about deoxyribose C1′–C2′ bonds can be related to the vicinal ^{1}H–^{1}H coupling constants $^3J_{H1'H2'}$ and $^3J_{H1'H2''}$ by eq 1.[77] In the case

$$^3J = 10.5 \cos^2 \Phi - 1.2 \cos \Phi \qquad (1)$$

of a C3′ exo sugar pucker, $^3J_{H1'H2'}$ = 6.1 Hz and $^3J_{H1'H2''}$ = 7.5 Hz; a C3′ endo sugar geometry has $^3J_{H1'H2'} = \approx 0$ and $^3J_{H1'H2''}$ = 7.5 Hz. Since the H1′ proton of a 2′-deoxyribose residue is part of an ABX spin system, the pure $^3J_{H1'H2'}$ or $^3J_{H1'H2''}$ value cannot be simply determined from the pattern of resonances. The sum $^3J_{H1'H2'} + {}^3J_{H1'H2''}$ can be obtained, however, since it corresponds to the separation of the outermost dominant transitions.[78] This observation affords a useful criterion for determining the sugar pucker. A C3′ endo geometry will have a sum of 13.6 Hz, and a C3′ exo pucker will have a sum of 7.5 Hz. All H1′ resonances of [d(ApGpGpCpCpT)]$_2$ have $\sum^3J$ values in the range 14.0 ± 1.0 Hz throughout the temperature range 2–65 °C and pH range 3.2–10.8 (35 °C). These values reveal a B-form DNA structure containing C2′ endo sugar conformations.

Structure of *cis*-[Pt(NH$_3$)$_2$\{d(ApGpGpCpCpT)-*N7-G(2),N7-G(3)*\}]. The *cis*-[Pt(NH$_3$)$_2$Cl$_2$] adduct of [d(ApGpGpCpCpT)]$_2$ adopts a single-stranded, predominantly base-destacked structure. The absence of any observable imino resonances at 2 °C indicates that the platinated adduct does not form a normal stable duplex structure with itself. Although the terminal A(1)·T(6) imino resonances were not observed in the unmodified oligonucleotide, the inner imino protons of the [–GpGpCpC–]$_2$ core were clearly visible. This difference suggests that the distortion induced by the *cis*-{Pt(NH$_3$)$_2$}$^{2+}$ moiety on the d(GpG) unit is severe enough to destabilize hydrogen bonding to the complementary d(CpC) unit at the hexanucleotide level. The inability of *cis*-[Pt-(NH$_3$)$_2$\{d(ApGpGpCpCpT)-*N7-G(2),N(7)-G(3)*\}] to form a duplex structure attests to the local disruptive influence of two neighboring, platinated d(GpG)·d(CpC) units. This phenomenon was also observed for *cis*-[Pt(NH$_3$)$_2$\{d(CpCpGpG)-*N7-G(3),N-(7)-G(4)*\}].[7] The destabilizing effect would also decrease the thermodynamic stability of *cis*-[Pt(NH$_3$)$_2$\{d(ApGpGpCpCpT)-*N7-G(2),N7-G(3)*\}]·d(ApGpGpCpCpT) relative to that of [d-(ApGpGpCpCpT)]$_2$, precluding the use of short platinated self-complementary oligonucleotides as models in the investigation of the effects of *cis*-[Pt(NH$_3$)$_2$Cl$_2$] on duplex DNA.

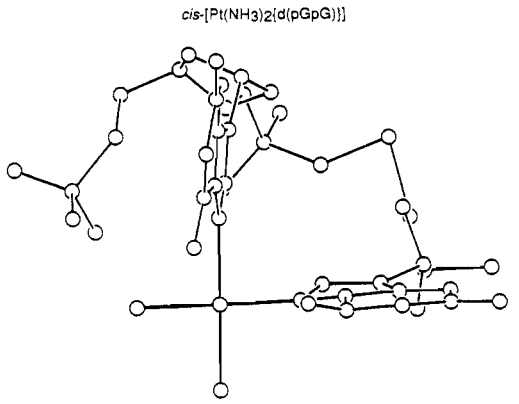

Figure 15. X-ray structure of *cis*-[Pt(NH$_3$)$_2$\{d(pGpG)\}], showing the local disruption of base stacking induced by *cis*-[Pt(NH$_3$)$_2$Cl$_2$] binding (drawn from the coordinates in ref 13).

The structural basis for these results have recently been elucidated. Specific details of the local disruption induced by *cis*-[Pt(NH$_3$)$_2$Cl$_2$] binding are provided by crystallographic studies of *cis*-[Pt(NH$_3$)$_2$\{d(pGpG)-*N7-G(1),N7-G(2)*\}][13] (Figure 15). The guanosine nucleotides adopt anti conformations with both O6 atoms situated over the same side of the platinum coordination plane. More significantly, the *cis*-{Pt(NH$_3$)$_2$}$^{2+}$ moiety alters the dihedral angle between coordinated bases, from ~0–10 to 76–87°, completely disrupting base stacking between the two guanosine residues. Molecular mechanics calculations on *cis*-{Pt(NH$_3$)$_2$}$^{2+}$ adducts of d(GpGpCpCpG*pG*pCpC)·d(GpGpCpCpGpGp-CpC), d(TpCpTpCpG*pG*pTpCpTpC)·d(GpApGpApCpC-pGpApGpA),[15] and d(ApG*pG*pCpCpT)[16] showed weakening or disruption of base pairs upon platination, as well as possible bending of the double helix. The latter has recently been experimentally established.[79] Although ^{1}H NMR studies have reported the observation of guanine imino resonances for *cis*-[Pt(NH$_3$)$_2$\{d(TpCpTpCpG*pG*pTpCpTpC)\}]·d(GpApGpA-pCpCpGpApGpA)[10,11] and *cis*-[Pt(NH$_3$)$_2$\{d-(GpApTpCpCpG*pG*pC)\}]·d(CpGpCpTpApGpGpCpCpG),[12] no evidence was given defining the specific nature of the base-pairing interactions. In view of the variety of potential hydrogen-bonding schemes predicted by molecular mechanics calculations and absence of X-ray structural data for platinated duplex oligonucleotides, details of the base-pair disruption induced by *cis*-[Pt(NH$_3$)$_2$Cl$_2$] binding remain to be established.

The temperature-dependent behavior of the chemical shifts of the nonexchangeable base protons (Figure 11) affords additional evidence for the single-stranded nature of *cis*-[Pt(NH$_3$)$_2$\{d-(ApGpGpCpCpT)\}]. Significant downfield shifting of all base resonances is observed in the spectrum of the platinated versus the spectrum of the unplatinated oligonucleotides, even for residues not directly coordinated to platinum. This phenomenon, which indicates decreased base-stacking interactions, is best exemplified by the two cytosine H6 resonances. The 0.236 ppm difference in chemical shift observed for the cytosine H6 resonances in [d(ApGpGpCpCpT)]$_2$ reflects the greater shielding ability of a neighboring 5′-purine versus that of a 5′-pyrimidine nucleotide. In the spectrum of the platinum(II) adduct, the two cytosine doublets have almost identical chemical shifts (environments) that show no temperature dependence (δ(93 °C) – δ(20 °C) ≤ 0.01

(76) Akasaka, K. *Biopolymers* **1974**, *13*, 2273–2280.
(77) Altona, C.; Sundaralingam, M. *J. Am. Chem. Soc.* **1973**, *95*, 2333–2344.
(78) Roberts, J. D. In *An Introduction to the Analysis of Spin-Spin Splitting in High Resolution Nuclear Magnetic Resonance Spectra*; W. A. Benjamin: New York, 1962.
(79) Rice, J.; Crothers, D.; Pinto, A.; Lippard, S. J. *Proc. Natl. Acad. Sci. U.S.A.*, in press.

ppm). Similar behavior is seen for the purine resonances, with adenine H2 and H8 and a guanine H8 resonance (resonance 4) all exhibiting a maximum temperature-dependent shift of less than 0.07 ppm.

An exception is guanine(3) H8, which shifts upfield by 0.30 ppm with increasing temperature, analogous to the results observed for *cis*-[Pt(NH$_3$)$_2$\{d(GpG)\}].[9] Changes in base-stacking interactions are not responsible for this effect, since the *cis*-{Pt(NH$_3$)$_2$}$^{2+}$ moiety fixes the two guanosine rings nearly orthogonal to one another (Figure 15).[13] Instead, the deshielding of guanine(3) H8 is attributed to an increase in the γ^+ population, a C4′–C5′ torsion angle of the -p-G(3) fragment, at lower temperatures. The net effect of this change in backbone conformation is to decrease the time-averaged distance between the C5′–O5′ bond and guanine(3) H8 with decreasing temperature, resulting in greater deshielding of the proton.[9]

Figure 5 shows the expanded H1′ region of the spectrum of *cis*-[Pt(NH$_3$)$_2$\{d(ApGpGpCpCpT)\}]. Four H1′ multiplets are resolved between 6.30 and 6.15 ppm. Slightly upfield, however, the region is more complex, containing two H1′ resonances (cytosine(5) H1′, guanine(2) H1′) and the two H5 doublets of cytosine. Although the guanine(2) H1′ resonance at 6.064 ppm overlaps with the cytosine(5) H5 doublet, the outer resonances of the H1′ multiplet can be observed and correspond to ^3J = 7.1 Hz, indicative of a C3′ endo sugar pucker. The switching of the 5′ sugar geometry of a *cis*-[Pt(NH$_3$)$_2$\{d(GpG)\}] unit has previously been reported for *cis*-[Pt(NH$_3$)$_2$\{d(GpG)\}],[9] *cis*-[Pt(NH$_3$)$_2$\{d(CpGpG)\}],[11] *cis*-[Pt(NH$_3$)$_2$\{d(TpCpTpCpGpGpTpCpTpC)\}],[10] and *cis*-[Pt(NH$_3$)$_2$\{d(TpGpGpCpCpA)\}].[42] One reason for this change is that the distance between the 3′- and 5′-phosphate groups in a sugar with C2′ endo is ~7.0 Å, while it is only 5.9 Å for a C3′ endo geometry. Since *cis*-{Pt(NH$_3$)$_2$}$^{2+}$ must bind covalently to both N7 atoms of adjacent guanosine bases, the latter conformation facilitates formation of the adduct. Recent calculations have shown the energy of this 5′–C3′ endo–3′–C2′ endo *cis*-[Pt(NH$_3$)$_2$\{d(GpG)\}] unit to be lower than the corresponding C2′–C2′ endo conformation.[15,16] The solid-state geometry of the 5′-deoxyribose rings in *cis*-[Pt(NH$_3$)$_2$\{d(pGpG)\}] was observed to be the same as that described by solution studies.[13,14] Switching of the 5′-residue pucker has not been observed for *cis*-[Pt(NH$_3$)$_2$\{d(GpNpG)\}] (N = A, C, or T), however, where the diammineplatinum(II) moiety forms a 1,3-adduct with an intervening base.[8] In this adduct, the deoxyribose groups of both the 5′- and 3′-nucleotides adopt a C2′ endo conformation, with the bases either undergoing rapid syn/anti interconversion or remaining in an intermediate conformation. In all cases reported, the central nucleotide appears to bulge out with the nucleotide maintaining its C2′ endo, anti conformation.

In the example of *trans*-[Pt(NH$_3$)$_2$\{d(ApGpGpCpCp)\}], the adenine(1) H1′ multiplet appears as a doublet with a $\sum^3J$ value of 7.4 Hz, indicating a C3′ endo sugar conformation.[22] The remaining H1′ multiplets have $\sum^3J$ values of 13.2 ± 0.8 Hz, typical of C2′ endo geometries. This result is consistent with the reported structures of *trans*-[Pt(NH$_3$)$_2$\{d(GpCpG)\}][80] and *trans*-[Pt(NH$_3$)$_2$\{d(GpTpG)\}].[81]

Summary and Possible Biological Consequences

The self-complementary hexanucleoside pentaphosphate [d(ApGpGpCpCpT)]$_2$ exists as a duplex oligonucleotide in solution, adopting C3′ exo (B-DNA) sugar conformations throughout a wide range of temperature and pH values. Although the terminal A(1)·T(6) base pairs are frayed at 37 °C, the [–GpGpCpC–]$_2$ core remains intact until 60.0 ± 3.0 °C. Upon reaction with the anticancer drug *cis*-[Pt(NH$_3$)$_2$Cl$_2$], only a single adduct is formed in any appreciable yield. This adduct is characterized as a nearest-neighbor *cis*-[Pt(NH$_3$)$_2$\{d(ApGpGpCpCpT)-*N7-G(2)*,-*N7-G(3)*\}] intrastrand cross-link and exists as a single-stranded base-destacked oligomer. No interstrand, guanine N7–O6 intrabase or *cis*-[Pt(NH$_3$)$_2$\{d(ApGpGpCpCpT)-*N7-A(1)*,*N7-G(2)*\}] adducts are observed.

These results allow a reappraisal of the ability of various *cis*-{Pt(NH$_3$)$_2$}–DNA adducts to form in vitro. Interstrand cross-links were the first adducts recognized in early biological studies.[82] Attempts to correlate the occurrence of this adduct with cytotoxicity, however, met with limited success.[83,84] There is considerable biological evidence arguing against the importance of such lesions,[85] a detailed discussion of which has appeared elsewhere.[4] The present work shows no evidence for interstrand adducts, even though the reaction was carried out under conditions favorable toward the formation of such species.

Several types of DNA intrastrand interactions have been proposed. An early model involved a guanine N7–O6 chelate.[21] To date, no direct evidence has been found to support this mode of binding.[86] The results reported here for *cis*-[Pt(NH$_3$)$_2$\{d(ApGpGpCpCpT)-*N7-G(2)*,*N7-G(3)*\}] clearly show the greater propensity of *cis*-[Pt(NH$_3$)$_2$Cl$_2$] to form a d(GpG) intrastrand cross-link, rather than an N7–O6 chelate.

Chromatographic analysis of nuclease-treated DNA platinated with *cis*-DDP indicated the presence of *cis*-[Pt(NH$_3$)$_2$\{d(pApG)\}] adducts.[19,87] No such product was observed in the present study. The absence of this adduct may be a direct consequence of the lack of a 5′-phosphate group, which might help initiate the formation of a *cis*-[Pt(NH$_3$)$_2$\{d(pApG)\}] cross-link. The preferential formation of the *cis*-[Pt(NH$_3$)$_2$\{d(GpG)\}] product results principally from kinetic effects. Competitive-binding studies between *cis*-[Pt(NH$_3$)$_2$Cl$_2$] and the four nucleic acid bases demonstrated the greater rate of Pt(II)–guanine complex formation.[45] It is important to note that the Pt/nucleotide levels used in the model investigations were substantially higher than is physiologically relevant. The observation of d(ApG) intrastrand cross-links may simply arise following initial saturation of the more preferred d(GpG) platinum binding sites, allowing secondary sites to react and produce biologically less frequent adducts. It remains to be determined, of course, whether such low-frequency adducts have any greater or different biological effects on DNA processing in vivo than the favored intrastrand d(GpG) cross-link.

The major differences between the binding of *cis*- and *trans*-[Pt(NH$_3$)$_2$Cl$_2$] to [d(ApGpGpCpCpT)]$_2$ are the product distribution and type of major adducts formed. While the cis isomer can form a nearest-neighbor cross-link, the trans isomer cannot. The major adduct formed with the trans isomer is similar to cis 1,3-adducts observed with GpXpG sequences, except for the sugar pucker of the 5′-nucleotide. The apparent structural similarity of these adducts argues against the importance of the 1,3-adduct, since only *cis*-DDP is active as a chemotherapeutic drug. The major significant difference between the binding of the two isomers is the unique ability of *cis*-DDP to form a nearest-neighbor cross-link.

The conclusions of this investigation agree with in vitro enzymatic and immunological studies implicating an intrastrand nearest-neighbor *cis*-[Pt(NH$_3$)$_2$] guanine N7, guanine N7 cross-link as the most important structure in the biochemistry of cisplatin with DNA.[4] Immunochemical studies have demonstrated the existence of this adduct, and the related d(ApG) cross-link, in the ascites fluid of L1210 tumor-bearing mice treated with *cis*-[Pt(NH$_3$)$_2$Cl$_2$] and in the white blood cells of cancer patients treated with *cis*-DDP.[89,90] Furthermore, since biologically inactive

(80) van der Veer, J. L.; Ligtvoet, G. J.; van den Elst, H.; Reedijk, J. *J. Am. Chem. Soc.* **1986**, *108*, 3860–3862.
(81) Gibson, D.; Lippard, S. J. *Inorg. Chem.* **1987**, *26*, 2275–2279.
(82) Roberts, J. J.; Pascoe, J. M. *Nature (London)* **1972**, *235*, 282–284.
(83) Zwelling, L. A.; Anderson, T.; Kohn, K. W. *Cancer Res.* **1979**, *39*, 365–369.
(84) Zwelling, L. A.; Michaels, S.; Schwartz, H.; Dobson, P. P.; Kohn, K. W. *Cancer Res.* **1981**, *41*, 640–649.
(85) Munchausen, L. L. *Proc. Natl. Acad. Sci. U.S.A.* **1974**, *71*, 4519–4522.
(86) Raudascl-Sieber, G.; Marzilli, L. G.; Lippert, B.; Shinozuka, K. *Inorg. Chem.* **1985**, *24*, 989–990.
(87) Fichtinger-Schepman, A. M. J.; van der Veer, J. L.; den Hartog, J. H. J.; Lohman, P. H. M.; Reedijk, J. *Biochemistry* **1985**, *24*, 707–713.
(88) Lippard, S. J.; Ushay, H. M.; Merkel, C. M.; Poirier, M. C. *Biochemistry* **1983**, *22*, 5165–5168.
(89) Reed, E.; Yuspa, S. H.; Zwelling, L. A.; Ozols, R. F.; Poirier, M. C. *J. Clin. Invest.* **1986**, *77*, 545–550.

trans-$[Pt(NH_3)_2Cl_2]$ is unable to form such adducts, a direct consequence of the stereochemical requirements of the trans square-planar metal center, this lesion uniquely demonstrates the requirement of cis stereochemistry. A deeper understanding of the molecular mechanism of action of *cis*-DDP will require detailed investigations of the dynamic structural changes induced by both *cis*- and *trans*-$[Pt(NH_3)_2Cl_2]$ upon binding to duplex oligonucleotides and the ability of cellular repair processes to recognize and eliminate these adducts.

Acknowledgment. This research was supported by U.S. Public Health Service Grant CA 34992 from the National Cancer Institute. We thank M. J. Gait for aid in the synthesis of [d(ApGpGpCpCpT)]$_2$ and C. J. Turner (Department of Chemistry, Columbia University) for helpful discussions with the spin-lattice relaxation measurements and NOESY experiments. The NOESY experiments were performed at the NMR Facility for Biomolecular Research located at the Francis Bitter National Magnet Laboratory at MIT. The NMR facility is supported by Grant No. RR00995 from the Division of Research Resources of the National Institutes of Health and by the National Science Foundation, under Contract No. C-670. We also thank Engelhard Corp. for a loan of K_2PtCl_4, from which *cis*-$[Pt(NH_3)_2Cl_2]$ was prepared.

(90) Fichtinger-Schepman, A. M. J.; van Oosterom, A. T.; Lohman, P. H. M.; Berends, F. *Cancer Res.* **1987**, *47*, 3000-3004.

Registry No. *cis*-DDP, 15663-27-1; d(ApGpGpCpCpT), 83026-06-6; *cis*-$[Pt(NH_3)_2\{d(ApGpGpCpCpT)$-*N7*-*G*(*2*),*N7*-*G*(*3*)$\}]$ (ammonium salt), 113132-29-9.

Contribution from the Institute of Inorganic Chemistry, University of Zürich, Winterthurerstrasse 190, 8057 Zürich, Switzerland

New Metal Complexes of the Antitumor Drug 6-Mercaptopurine. Syntheses and X-ray Structural Characterizations of Dichloro(6-mercaptopurinium)copper(I), Dichlorotetrakis(6-mercaptopurine)cadmium(II), and Bis(6-mercaptopurinato)cadmium(II) Dihydrate

Erich Dubler* and Ernst Gyr

Received September 17, 1987

Three new metal complexes of the antitumor drug 6-mercaptopurine ($C_5H_4N_4S$, MP) have been crystallized from aqueous solutions. $Cu^I(MP^+)Cl_2$ is triclinic, space group $P\bar{1}$, with a = 7.435 (7) Å, b = 8.848 (5) Å, c = 7.271 (3) Å, α = 109.13 (3)°, β = 99.75 (7)°, γ = 96.83 (7)°, V = 437.5 (12) Å^3, and Z = 2, and is refined to R = 0.028. In contrast to the hydrated complex $Cu^I(MP^+)Cl_2 \cdot H_2O$, where S-bridged dimers occur, the anhydrate exhibits a new structure with Cl-bridged dimers of the type $[Cu_2(MP^+)_2Cl_4]$. MP^+ is protonated at N(1), N(7), and N(9) and binds to copper through its sulfur atom only. The copper(I) coordination is distorted tetrahedral with Cu-S = 2.221 (1) Å and Cu-Cl = 2.465 (1) and 2.493 (1) Å (bridging) and 2.251 (1) Å (terminal). $Cd^{II}(MP)_4Cl_2$ is triclinic, space group $P\bar{1}$, with a = 8.083 (2) Å, b = 11.904 (3) Å, c = 7.374 (2) Å, α = 99.04 (2)°, β = 101.30 (2)°, γ = 91.53 (2)°, V = 685.9 (6) Å^3, and Z = 1, and is refined to R = 0.027. The structure contains one isolated octahedral $[Cd(MP)_2Cl_2]$ unit and two noncoordinating MP molecules per cell. The two crystallographically independent MP molecules both are protonated at N(1) and at N(9), but not at N(7). The coordinating molecule acts as a S/N(7) bidentate chelating ligand. Bonding distances are Cd-S = 2.622 (1) Å, Cd-N = 2.366 (1) Å, and Cd-Cl = 2.719 (1) Å. $Cd^{II}(MP^-)_2 \cdot 2H_2O$ is triclinic, space group $P\bar{1}$, with a = 3.918 (3) Å, b = 9.371 (3) Å, c = 11.162 (5) Å, α = 67.89 (3)°, β = 84.40 (4)°, γ = 76.84 (4)°, V = 369.7 (4) Å^3, and Z = 1, and is refined to R = 0.044. This complex exhibits a new polymeric structure type with infinite chains of Cd atoms linked by bridging S atoms. Cd is octahedrally coordinated by four S and two N atoms of the S/N(7)-chelating MP ligand. Bonding distances are Cd-S = 2.689 (1) and 2.868 (1) Å and Cd-N = 2.283 (3) Å. A detailed analysis of bond lengths and angles of MP in its neutral, deprotonated, or protonated form is given. Metal coordination at N(7) induces changes in the geometry of the imidazole moiety of MP similar to, but much smaller than, those induced by protonation at N(7).

Introduction

6-Mercaptopurine ($C_5H_4N_4S$, MP) is a synthetic thio analogue of the natural purine hypoxanthine and is used as an established clinical agent for the therapy of human leukemias. Its antimetabolitic mechanism of action is believed to be due to its being converted intracellularly to the corresponding ribonucleotide, which in turn suppresses purine synthesis and inhibits different purine metabolic processes.[1]

There are different interesting aspects of the formation and reactivity of MP metal complexes. On the basis of the discovery of the anticancer activity of cisplatin (*cis*-dichlorodiammineplatinum(II)) by Rosenberg in 1969,[2] new metal coordination compounds, including those with drugs acting as ligands, have been screened in regard to their anticancer activity. It has been found that some metal complexes of MP, especially those of platinum and palladium, show antitumor activity, which in some cases is even enhanced with respect to the activity of the free ligand.[3] In addition, coordination metal complexes of drugs generally may be of importance in the design of repository, slow-release, or long-acting drugs. According to Hansen et al.,[4] divalent metal ions, e.g. copper(II), may increase the amount of MP binding to yeast RNA. In a study of the interaction between MP, Cu^{2+}, and the enzyme xanthine oxidase, it has been found that Cu^{2+} inhibits the enzyme, whereas MP could protect as well as reverse this enzyme inhibition, and it has been suggested that the formation of a stable Cu-MP complex is an additional mechanism of action of MP with reference to its antiinflammatory properties.[5]

The formation of MP complexes of Mg(II) and Ca(II), of the transition metals Mn(II), Fe(II), Co(II), Co(III), Ni(II), Cu(I), Cu(II), Zn(II), Ru(II), Ru(III), Rh(III), Pd(II), Ag(I), Cd(II),

* To whom correspondence should be addressed.

(1) Jewers, K. In *Progress in Drug Research*; Jucker, E., Ed.; Birkhäuser: Basel, Switzerland, 1981; Vol. 25, p 275.
(2) Rosenberg, B.; Van Camp, L.; Trosko, J. E.; Mansour, V. H. *Nature (London)* **1969**, *222*, 385.
(3) (a) Kirschner, S.; Wei, Y. K.; Francis, D.; Bergman, J. G. *J. Med. Chem.* **1969**, *9*, 369. (b) Skinner, S. M.; Swatzell, J. M.; Lewis, R. W. *Res. Commun. Chem. Pathol. Pharmacol.* **1978**, *19*, 165. (c) Das, M.; Livingstone, S. E. *Br. J. Cancer* **1978**, *38*, 325.
(4) Hansen, H. J.; Bennett, S. J.; Nadler, S. B. *Arch. Biochem. Biophys.* **1962**, *98*, 379.
(5) Kela, U.; Vijayvargiya, R. *Biochem. J.* **1981**, *193*, 799.

0020-1669/88/1327-1466$01.50/0